Article

Palladium-Catalyzed Formylation of Aryl Bromides: Elucidation of the Catalytic Cycle of an Industrially Applied Coupling Reaction

Alexey G. Sergeev, Anke Spannenberg, and Matthias Beller

J. Am. Chem. Soc., **2008**, 130 (46), 15549-15563 • DOI: 10.1021/ja804997z • Publication Date (Web): 29 October 2008

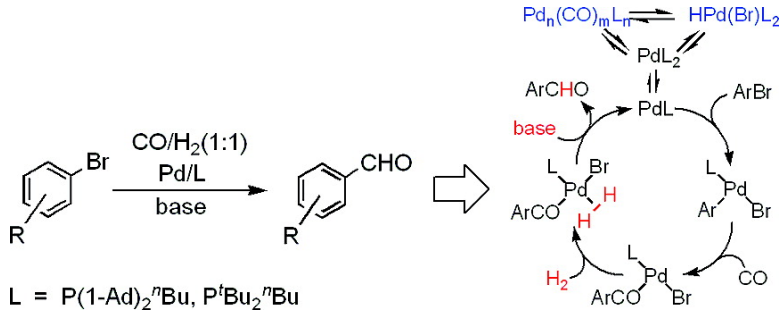

More About This Article

Additional resources and features associated with this article are available within the HTML version:

- Supporting Information
- Access to high resolution figures
- Links to articles and content related to this article
- Copyright permission to reproduce figures and/or text from this article

View the Full Text HTML

Journal of the American Chemical Society is published by the American Chemical Society. 1155 Sixteenth Street N.W., Washington, DC 20036

J|A|C|S
ARTICLES

Published on Web 10/29/2008

Palladium-Catalyzed Formylation of Aryl Bromides: Elucidation of the Catalytic Cycle of an Industrially Applied Coupling Reaction

Alexey G. Sergeev, Anke Spannenberg, and Matthias Beller*

Leibniz-Institut für Katalyse e.V. an der Universität Rostock, Albert-Einstein-Strasse 29a, 18059 Rostock, Germany

Received July 14, 2008; E-mail: matthias.beller@catalysis.de

Abstract: The first comprehensive study of the catalytic cycle of the palladium-catalyzed formylation of aryl bromides with synthesis gas (CO/H_2, 1:1) is presented. The formylation in the presence of efficient ($Pd/PR_2{}^nBu$, R = 1-Ad, ^tBu) and nonefficient (Pd/P^tBu_3) catalysts was investigated. The main organometallic complexes involved in the catalytic cycle were synthesized and characterized, and their solution chemistry was studied in detail. Comparison of stoichiometric and catalytic reactions using $P(1\text{-}Ad)_2{}^nBu$, the most efficient ligand known for the formylation of aryl halides, led to two pivotal results: (1) The corresponding carbonylpalladium(0) complex $[Pd_n(CO)_mL_n]$ and the respective hydrobromide complex $[Pd(Br)(H)L_2]$ are resting states of the active catalyst, and they are not directly involved in the catalytic cycle. These complexes maintain the concentration of most active [PdL] species at a low level throughout the reaction, making oxidative addition the rate-determining step, and provide high catalyst longevity. (2) The product-forming step proceeds via base-mediated hydrogenolysis of the corresponding acyl complex, e.g., $[Pd(Br)(p\text{-}CF_3C_6H_4CO)\{P(1\text{-}Ad)_2{}^nBu\}]_2$ (**8**), under mild conditions (25−50 °C, 5 bar). Stoichiometric studies using the less efficient Pd/P^tBu_3 catalyst resulted in the isolation and characterization of the first stable three-coordinated neutral acylpalladium complex, $[Pd(Br)(p\text{-}CF_3C_6H_4CO)(P^tBu_3)]$ (**10**). Hydrogenolysis of **10** needed significantly more drastic conditions compared to that of dimeric **8**. In the presence of amine base, complex **10** gave a catalytically inactive diamino acyl complex, which explains the low activity of the Pd/P^tBu_3 catalyst formylation of aryl bromides.

Introduction

The palladium-catalyzed formylation of aryl halides constitutes an attractive method for the preparation of aromatic aldehydes. In general, synthetic protocols for catalytic formylation of aryl halides use combinations of CO[2,3] or acetic formic anhydride[1] as carbonylation agents and silyl[2] or tin[3] hydrides as well as formate salts[4] as hydrogen donors. Unfortunately, side reactions such as reductive dehalogenation, limited functional group tolerance, high catalyst loadings, and environmentally nonbenign reagents restricted this methodology. During our search for more reliable protocols to overcome these limitations, we turned our attention to synthesis gas (CO/H_2 mixture), the simplest and cheapest formylation agent widely used in numerous industrial applications. Before our work, only a few reports on the use of synthesis gas for formylation of aryl halides were published. In all of them, $[Pd(PPh_3)_2Cl_2]$ was employed as catalyst, and the reactions proceeded at high pressure (30−100 bar) and temperature (125−150 °C).[5,6] Recently, we demonstrated that a catalytic system comprising $Pd(OAc)_2$ and $P(1\text{-}Ad)_2{}^nBu$ (cataCXium A, Evonik Degussa GmbH) enables a more efficient (0.1−0.25 mol % of palladium) formylation of aryl bromides under milder conditions (5 bar pressure of synthesis gas).[7] The high selectivity and efficiency of the catalytic system allowed it to be used in the first industrial-scale formylation of aryl halides (>1000 kg scale).

Notably, $P(1\text{-}Ad)_2{}^nBu$ is also known to be an efficient ligand for other palladium-catalyzed carbonylations, e.g., alkoxycarbonylation of aryl bromides[8] and carbonylative Suzuki coupling,[9] as well as Buchwald−Hartwig aminations[10] and Mizoroki−Heck,[11] Suzuki,[12] Sonogashira,[13] and ketone arylation reactions.[14] Comparing the catalytic performance of $P(1\text{-}Ad)_2{}^nBu$ with that of symmetrically substituted bulky phosphines

(1) Cacchi, S.; Fabrizi, G.; Goggiamani, A. *J. Comb. Chem.* **2004**, *6*, 692.
(2) Pri-Bar, I.; Buchman, O. *J. Org. Chem.* **1984**, *49*, 4009.
(3) (a) Baillargeon, V. P.; Stille, J. K. *J. Am. Chem. Soc.* **1974**, *96*, 7761. (b) Misumi, Y.; Ishii, Y.; Hidai, M. *Organometallics* **1995**, *14*, 1770.
(4) Ben-David, Y.; Portnoy, M.; Milstein, D. *J. Chem. Soc., Chem. Commun.* **1989**, 1816.
(5) First use of synthesis gas in palladium-catalyzed formylation: Schoenberg, A.; Heck, R. F. *J. Am. Chem. Soc.* **1974**, *96*, 7761.
(6) Palladium-catalyzed formylation of aryl halides activated with coordination with tricarbonylchromium: Mutin, R.; Lucas, C.; Thivolle-Cazat, J.; Dufaud, V.; Dany, F.; Basset, J. M. *J. Chem. Soc., Chem. Commun.* **1988**, 896.
(7) (a) Klaus, S.; Neumann, H.; Zapf, A.; Strübing, D.; Hübner, S.; Almena, J.; Riermeier, T.; Groβ, P.; Sarich, M.; Krahnert, W.-R.; Rossen, K.; Beller, M. *Angew. Chem., Int. Ed.* **2006**, *45*, 154. (b) Brennführer, A.; Neumann, H.; Klaus, S.; Riermeier, T.; Almena, J.; Beller, M. *Tetrahedron* **2007**, *65*, 6252.
(8) Neumann, H.; Brennführer, A.; Groβ, P.; Riermeier, T.; Almena, J.; Beller, M. *Adv. Synth. Catal.* **2006**, *348*, 1255.
(9) Neumann, H.; Brennführer, A.; Beller, M. *Chem. Eur. J.* **2008**, *14*, 3645.
(10) (a) Ehrentraut, A.; Zapf, A.; Beller, M. *J. Mol. Catal.* **2002**, *182*−*183*, 515. (b) Tewari, A.; Hein, M.; Zapf, A.; Beller, M. *Tetrahedron* **2005**, *61*, 9705.
(11) Ehrentraut, A.; Zapf, A.; Beller, M. *Synlett* **2000**, 1589.

Scheme 1. Proposed Catalytic Cycle for the Pd-Catalyzed Formylation of Aryl Bromides with Synthesis Gas

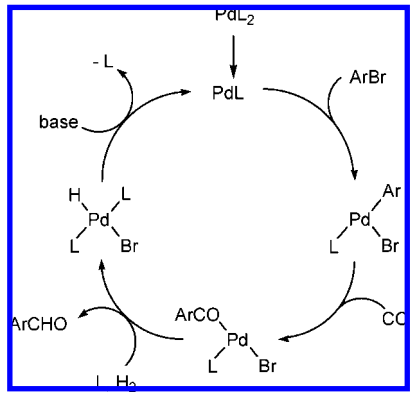

such as PCy_3 and P^tBu_3, significant differences are observed.[7] Hence, the specific substitution pattern including two bulky alkyl groups and the *n*-butyl tail seems to be essential for the high efficiency of the catalytic system. Replacement of the *n*-butyl tail with other substituents such as methyl or benzyl led to a significant drop in activity. In order to understand these issues, we studied the synthesis and organometallic chemistry of palladium complexes bearing unsymmetrically substituted bulky alkylphosphines. More specifically, we focused our attention on the organometallic elementary steps of the catalytic formylation of aryl halides in the presence of $P(1\text{-}Ad)_2{}^nBu$-derived palladium catalysts, which surpass the efficiency of all known catalytic systems. To the best of our knowledge, no systematic stoichiometric studies on palladium-catalyzed formylation of aryl halides have been reported previously. To date, only two examples concerning the product-forming step, namely, hydrogenolysis of acylpalladium complexes of the type $[Pd\{(O)CR\}(X)(PPh_3)_2]$, where X = Hal[15] or OC(O)R′,[16] have been published. The same is partly true for carbonylations of aryl halides in general: despite the importance and wide use of palladium complexes with bulky alkylphosphine ligands, there is a lack of mechanistic details about these complexes involved in the catalytic cycle.[17]

In the present paper we describe the synthesis, characterization, and crystal structures as well as the solution chemistry of most of the complexes involved in the palladium-catalyzed formylation of aryl halides with synthesis gas. All key steps of the catalytic cycle were investigated one by one, and the results of these studies were combined with the data on the catalytic reaction. As a result, a catalytic cycle for palladium-catalyzed formylation of aryl halides is established, which contributes to a better understanding of palladium-catalyzed carbonylations in general.

Results and Discussion

As a model for our stoichiometric studies, we chose the catalytic formylation of 4-bromobenzotrifluoride in the presence of three bulky phosphine ligands: $P(1\text{-}Ad)_2{}^nBu$, $P^tBu_2{}^nBu$, and P^tBu_3. The reactions were carried out using a combination of 0.25 mol % of palladium acetate and 0.75 mol % of the ligand in the presence of TMEDA as a base in toluene at 100 °C and 5 bar pressure of synthesis gas (a 1:1 CO/H_2 mixture) (eq 1), which is comparable to the industrially applied conditions.

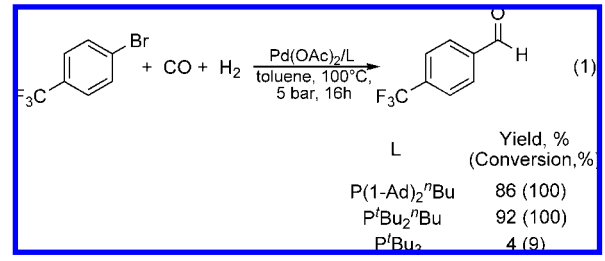

Use of $Pd/P(1\text{-}Ad)_2{}^nBu$, the commercially applied formylation catalyst, resulted in 4-trifluorobenzaldehyde in 86% yield.[7] A catalyst based on $P^tBu_2{}^nBu$ of similar structure also gave the corresponding aldehyde in high yield (92%). In contrast, application of the P^tBu_3-ligated catalyst led to low conversion and only 4% yield of the product! Apparently, the nature of the bulky substituents R in $PR_2{}^nBu$ does not appreciably change the catalytic activity, whereas replacement of the *n*-butyl group led to severe deterioration of the catalyst performance. In order to understand this different behavior, we studied all elementary steps of the catalytic cycle using this set of ligands.

As the basis for our work, the generally accepted mechanism shown in Scheme 1 was used. It includes oxidative addition of the aryl bromide to the active palladium(0) species, migratory insertion of CO into the Ar−Pd bond, and hydrogenolysis of the resulting acyl complex to give the desired aldehyde. Finally, the formed palladium hydrobromide complex is regenerated to Pd(0) after reaction with base.

1. Synthesis and Structure of Palladium(0) Complexes. Initially, palladium(0) complexes $[PdL_2]$ were synthesized by reaction of [AllylPdCp] with an excess of $P(1\text{-}Ad)_2{}^nBu$ or $P^tBu_2{}^nBu$ in heptane solution (eq 2). Complex **1** directly precipitated from the reaction mixture and was isolated by simple filtration followed by crystallization from a toluene/methanol mixture to give white crystals in 77% yield. The palladium(0) complex of $P^tBu_2{}^nBu$ (**2**) was isolated in 82% yield via evaporation of the reaction mixture and subsequent crystallization from a mixture of ether/methanol.

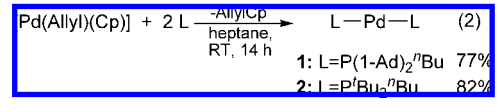

The structure of the obtained complexes was confirmed by X-ray analysis (Figures 1 and 2). Selected bond lengths and angles are given in Table 1.

Complex **2** shows a linear P1−Pd1−P1′ angle (180°), whereas **1** exhibits a slightly bent geometry with a P1−Pd1−P2 angle of 172°. Interestingly, the conformations of the different alkyl substituents along the P−Pd−P axis in both complexes vary markedly. Complex **2** adopts a staggered conformation

(12) (a) Zapf, A.; Ehrentraut, A.; Beller, M. *Angew. Chem. Int. Ed* **2000**, *39*, 4153. (b) Tewari, A.; Hein, M.; Zapf, A.; Beller, M. *Synthesis* **2004**, 935.
(13) (a) Köllhofer, A.; Pullmann, T.; Plenio, H. *Angew. Chem., Int. Ed.* **2003**, *42*, 1056. (b) Hillerich, J.; Plenio, H. *Chem. Commun.* **2003**, 3024. (c) Remmele, H.; Köllhofer, A.; Plenio, H. *Organometallics* **2003**, *22*, 4098. (d) Köllhofer, A.; Plenio, H. *Chem. Eur. J.* **2003**, *9*, 1416.
(14) Ehrentraut, A.; Zapf, A.; Beller, M. *Adv. Synth. Catal.* **2002**, *344*, 209.
(15) Heaton, B. T.; Hébert, S. P. A.; Iggo, J. A.; Metz, F.; Whyman, R. *J. Chem. Soc., Dalton Trans.* **1993**, 3081.
(16) Nagayama, K.; Kawastaka, F.; Sakamoto, M.; Shimizu, I.; Yamamoto, A. *Bull. Chem. Soc. Jpn.* **1999**, *72*, 573.
(17) Martinelli, J. R.; Clark, T. P.; Watson, D. A.; Munday, R. H.; Buchwald, S. L. *Angew. Chem., Int. Ed.* **2007**, *46*, 8460–8463.

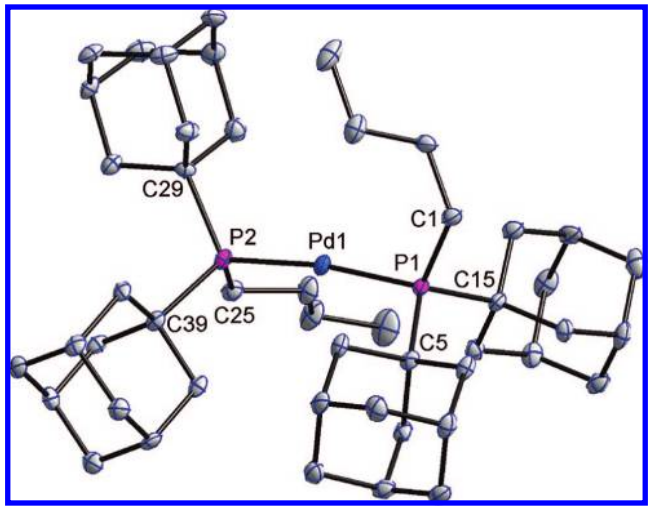

Figure 1. Molecular structure of **1**.[26] Hydrogen atoms are omitted for clarity. The thermal ellipsoids correspond to 30% probability.

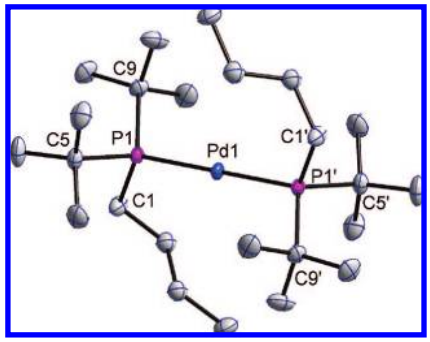

Figure 2. Molecular structure of **2**. Hydrogen atoms are omitted for clarity. The asymmetric unit contains half of the molecule; the remaining part is generated by the following symmetry operator: $-x + 2, -y, -z + 1$. The thermal ellipsoids correspond to 30% probability.

Table 1. Selected Bond Lengths (Å) and Angles (°) for **1** and **2**

complex **1**[26]		complex **2**	
Pd1−P1	2.286(2)	Pd1−P1	2.2850(4)
Pd1−P2	2.286(2)	Pd1−P1′	2.2849(4)
P2−Pd1−P1	172.18(5)	P1−Pd1−P1′	179.999(1)
α[a]	15.4(3)	C1−P1−P1′−C1′	180.0(1)
β[b]	5.1(1)	C5−P1−P1′−C5′	180.0(1)
γ[c]	17.1(3)	C9−P1−P1′−C9′	180.0(1)

[a] Angle between planes defined by C1,P1,P2 and P1,P2,C29 respectively. [b] Angle between planes defined by C5,P1,P2 and P1,P2,C39 respectively. [c] Angle between planes defined by C15,P1,P2 and P1,P2,C25 respectively.

which is typical for the majority of bisphosphine palladium(0) complexes,[18,19] including $[Pd(P^tBu_3)_2]$.[20] In contrast, complex **1** takes an eclipsed arrangement of substituents about the P1−Pd1−P2 direction, which is known for $[Pd(PCy_3)_2]$[21] and $[Pd(PPh^tBu_2)_2]$.[22] As for geometries of **1** and of **2**, the effect of steric factors on the conformation should be ruled out due to

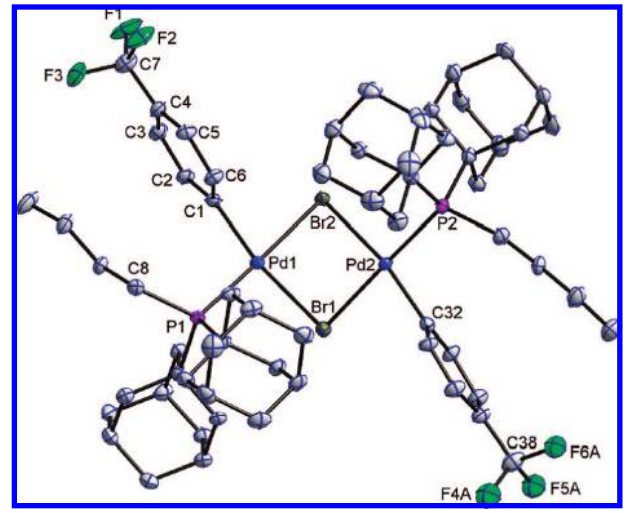

Figure 3. Molecular structure of **3**·$4C_7H_8$.[26] Hydrogen atoms are omitted for clarity. The thermal ellipsoids correspond to 30% probability.

Table 2. Selected Bond Lengths (Å) and Angles (°) for **3**·$4C_7H_8$[26]

Pd1−Br1	2.5618(10)	C1−Pd1−P1	91.8(1)
Pd1−Br2	2.5326(9)	C1−Pd1−Br1	169.5(1)
Pd1−C1	2.012(4)	Pd1−Br1−Pd2	81.55(4)
Pd1−P1	2.302(1)	C8−P1−Pd1−C1	−9.8(2)
Br1−Pd1−Br2	83.03(4)	α[a]	120.16(7)
P1−Pd1−Br1	98.70(5)	β[b]	79.2(1)

[a] Folding angle between planes defined by P1,C1,Pd1,Br1,Br2 and P2,C32,Pd2,Br1,Br2 respectively. [b] Angle between planes defined by P1,C1,Pd1,Br1,Br2 and C1−C6, respectively.

the large distance between substituents bound to different phosphorus atoms. Furthermore, complex **1** bearing the bulky 1-adamantyl groups adopts an eclipsed arrangement, whereas **2** having the less bulky *tert*-butyl substituents prefers to take up a staggered conformation.

2. Synthesis, Structure, and Solution Behavior of Arylpalladium Bromide Complexes. Next, oxidative addition of aryl bromides to the palladium(0) complexes **1** and **2** led to arylpalladium bromide dimers **3** and **4** in 55−80% isolated yields. Both complexes precipitated from the reaction mixture or after addition of heptane (eq 3).

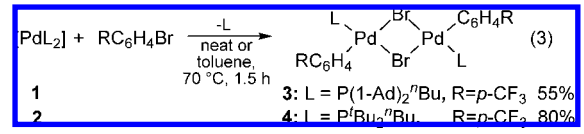

It is noteworthy that ^{31}P NMR spectra of the reaction mixtures showed that the dimeric complexes are present in solution only in small concentrations, whereas the corresponding monomeric bisphosphine arylpalladium complexes are the major species. Details on the reversible reaction of dimeric complexes **3** and **4** with phosphine ligands, as well as the structure of the corresponding bisphosphine complexes, are discussed below. In contrast to reactions with **1** and **2** (eq 3), the oxidative addition to $[Pd(P^tBu_3)_2]$ gave monomeric T-shaped species as shown by Hartwig.[23,24] Unlike the synthesis of complexes **3** and **4**, the reaction toward $[Pd(Br)(p\text{-}CF_3C_6H_4)(P^tBu_3)]$ (**5**) (eq 4) was

(18) (a) Reid, S. M.; Boyle, R. C.; Mague, J. T.; Fink, M. J. *J. Am. Chem. Soc.* **2003**, *125*, 7816. (b) Weng, Z.; Teo, S.; Koh, L. L.; Hor, T. S. A. *Organometallics* **2004**, *23*, 4342. (c) Grotjahn, D. B.; Gong, Y.; Zakharov, L.; Golen, J. A.; Rheingold, A. L. *J. Am. Chem. Soc.* **2006**, *128*, 438.
(19) Paul, F.; Patt, J.; Hartwig, J. F. *Organometallics* **1995**, *14*, 3030.
(20) Tanaka, M. *Acta Crystallogr.* **1992**, *C48*, 739.
(21) Immirzi, A.; Musco, A. *Chem. Commun.* **1974**, 400.
(22) (a) Matsumoto, M.; Yoshioka, H.; Nakatsu, K.; Yoshida, T.; Otsuka, S. *J. Am. Chem. Soc.* **1974**, *96*, 3322. (b) Otsuka, S.; Yoshida, T.; Matsumoto, M.; Nakatsu, K. *J. Am. Chem. Soc.* **1976**, *98*, 5850.

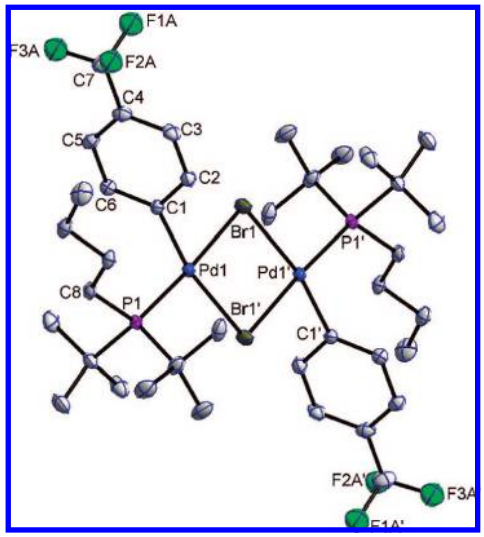

Figure 4. Molecular structure of **4**. Hydrogen atoms are omitted for clarity. The asymmetric unit contains half of the molecule; the remaining part is generated by the following symmetry operator: $-x + 1, -y + 1, -z + 1$. The thermal ellipsoids correspond to 30% probability.

Table 3. Selected Bond Lengths (Å) and Angles (°) for **4**

Pd1−C1	1.984(3)	Br1−Pd1−Br1′	82.85(1)
Pd1−P1	2.2891(8)	C1−Pd1−P1	90.04(9)
Pd1−Br1	2.5176(4)	C8−P1−Pd1-C1	1.1(2)
Pd1−Br′	2.5812(4)	Pd1−Br−Pd1′	97.15(1)
C1−Pd1−Br1	85.86(9)	α[a]	180.0(1)
P1−Pd1−Br1′	101.26(2)	β[b]	72.76(9)

[a] Folding angle between planes defined by P1,C1,Pd1,Br1,Br1′ and P1′,C1′,Pd1′,Br1,Br1′ respectively. [b] Angle between planes defined by P1,C1,Pd1,Br1,Br1′ and C1−C6 respectively.

accompanied with the formation of several side products presumably due to decomposition of **5**.[25] Therefore, the reaction time should be minimized to obtain acceptable yields of **5**.

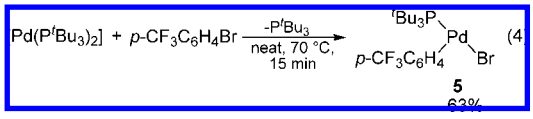

Complexes **3** and **4**, assumed to be involved in the catalytic cycle, exist as dimers both in the solid state and in solution, as shown by X-ray and NMR data.[26] Molecular structures of **3** and **4** are depicted in Figures 3 and 4, and selected bond lengths and angles are given in Tables 2 and 3, respectively.

Both structures show a *trans* geometry of the complexes with two palladium square planar units linked by two bromine atoms. The units are located to each other at a folding angle of 120.2° in complex **3** and 180° in complex **4**.[27] The complexes exhibit a peculiar arrangement of the substituents about P−Pd bonds: in either of the two palladium square planar units the *n*-butyl group of the coordinated phosphine and the aromatic group bound to palladium are in eclipsed positions, so that the *n*-butyl group lies roughly parallel to the plane of the aromatic ring and the γ-methylene group is placed nearly above the center of the ring. Such a conformation might be explained on the basis of steric effects.[28] In solution, complexes **3** and **4** exhibit fluxional behavior due to *cis*−*trans* isomerization and restricted rotation about the Pd−P bonds. At room temperature the $^{31}P\{^1H\}$ NMR spectra of the complexes in THF-d_8 displayed two broad singlets at 47.4 and 44.4 ppm for **3** and 51.6 and 50.4 ppm for **4** in a ratio of 74:26 and 60:40, respectively. The signals of major and minor forms are assigned to *trans* and *cis* isomers of dimers, respectively.[29] Domination of the *trans* form in THF is explained by steric reasons. A larger *trans*-to-*cis* ratio for **3** (74:26) as compared to that of **4** (60:40) is a consequence of the increased steric bulk of P(1-Ad)$_2{}^n$Bu compared to P^{t}Bu$_2{}^n$Bu and the nonplanar structure of **3** that might additionally increase the steric strain in the *cis* form. In contrast to the $^{31}P\{^1H\}$ NMR spectra of **3** and **4**, displaying two distinctive signals for *cis* and *trans* forms, in the proton spectra both forms are in fast exchange, as indicated by the presence of only one pair of broadened aromatic doublets at 7.59 and 7.11 ppm for **3** and 7.59 and 7.13 ppm for **4**. On cooling of the solutions to −40 (complex **3**) and −60 °C (complex **4**), these broadened signals resolved into two pairs of doublets corresponding to the *cis* and *trans* forms. A closer look at the aliphatic part of the proton spectra revealed that both isomers of **3** and **4** show pronounced upfield shifts of the *n*-butyl protons. This effect is explained by the aromatic ring current effect[30] if we suppose that both *cis* and *trans* forms of the complexes possess the same eclipsed orientations of *n*-butyl groups and aromatic rings that were found in the solid state. The shielding of the methylene protons is also seen by comparison of the ^1H NMR spectra of arylpalladium complexes **3** and **4** with those of the analogous bisphosphine palladium(0) complexes **1** and **2** (Table 4).

Chemical shifts of the adamantyl and *tert*-butyl protons are changed only slightly on going from [PdL$_2$] to [Pd(Ar)(Br)L]$_2$, whereas signals of the *n*-butyl protons are shifted by up to 1.3 ppm toward high field. Moreover, the γ-methylene protons of the *n*-butyl group show signals at even higher field than the corresponding methyl protons! This is a result of the closer location of γ-methylene protons to the centers of the aromatic rings, where the shielding has a peak value.

(23) Stambuli, J. P.; Bühl, M.; Hartwig, J. F. *J. Am. Chem. Soc.* **2002**, *124*, 9346.
(24) Stambuli, J. P.; Incarvito, C. D.; Bühl, M.; Hartwig, J. F. *J. Am. Chem. Soc.* **2004**, *126*, 1184.
(25) Barrios-Landeros, F.; Carrow, B. P.; Hartwig, J. F. *J. Am. Chem. Soc.* **2008**, *130*, 5842.
(26) Recently we reported elucidation of dimeric structure of P(1-Ad)$_2{}^n$Bu-ligated arylpalladium bromide complexes in solution as well as the existence of *cis*−*trans* equilibrium between dimers: Sergeev, A. G.; Zapf, A.; Spannenberg, A.; Beller, M. *Organometallics* **2008**, *27*, 297.
(27) Most dimeric arylpalladium complexes possess nearly coplanar orientations of the two palladium square planes. For selected structures, see: (a) Dufaud, V.; Thivolle-Cazat, J.; Basset, J.-M.; Mathieu, R.; Jaud, J.; Waissermann, J. *Organometallics* **1991**, *10*, 4005. (b) Paul, F.; Patt, J.; Hartwig, J. F. *J. Am. Chem. Soc.* **1994**, *116*, 5969. (c) Lin, S.-T.; Cheo, H.-S.; Liu, L.-S.; Wang, J.-C. *Organometallics* **1997**, *16*, 1803. (d) Marshall, W. J.; Young, R. J., Jr.; Grushin, V. V. *Organometallics* **2001**, *20*, 523. (e) Bartolomé, C.; Espinet, P.; Martín-Alvarez, J. M.; Villafañe, F. *Eur. J. Inorg. Chem.* **2003**, 3127. (f) Teo, S.; Weng, Z.; Hor, T. S. A. *Organometallics* **2006**, *25*, 1199.
(28) For comparison of steric parameters of substituents in organometallic compounds: White, D. P.; Anthony, J. C.; Oyefeso, A. O. *J. Org. Chem.* **1999**, *64*, 7707, and references therein.
(29) On cooling of the solutions of **3** and **4** to −60 and −80 °C, these signals sharpen and two additional marginal singlets appear. New signals probably correspond to various minor conformers of *cis* and *trans* form.
(30) (a) March, J. *Advanced Organic Chemistry. Reactions, Mechanisms, and Structure*, 6th ed.; John Wiley & Sons: New York, 2007; pp 54−92. (b) Chen, J.; Cammers-Goodwin, A. *Eur. J. Org. Chem.* **2003**, 3861. (c) Pascal, R. A., Jr.; Winans, C. G.; Engen, D. V. *J. Am. Chem. Soc.* **1989**, *111*, 3007. (d) Boekelheide, V. *Pure Appl. Chem.* **1975**, *44*, 751.

Table 4. ^{1}H NMR Chemical Shifts of the *n*-Butyl Protons in Arylpalladium Complexes **3** and **4** and Corresponding Palladium(0) Complexes **1** and **2**

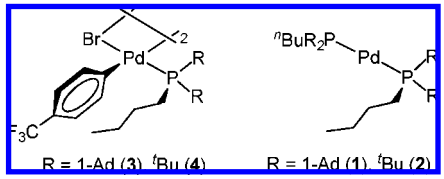

complex	δH(CH_3), ppm	δH(γ-CH_2), ppm	δH(β-CH_2), ppm	δH(α-CH_2), ppm
3[a]	0.62	0.43	0.98	1.23
1[a]	1.09	1.73	1.98	1.46
4[b]	0.55	0.42	0.99	1.42
2[b]	0.91	1.61	1.77	1.44

[a] ^{1}H NMR spectrum recorded in toluene-d_8 at −36 °C. [b] ^{1}H NMR spectrum recorded in THF-d_8 at −60 °C.

The ^{31}P{^{1}H} NMR spectra of the reaction mixtures of **1** and **2** with 4-bromobenzotrifluoride (eq 3) showed formation of monomeric bisphosphine aryl complexes as the main species instead of dimers **3** and **4** that were finally isolated as products via precipitation. This implies that the dimer complexes reversibly react with phosphines to give the corresponding bisphosphine species. To prove this assumption, dimer **3** was reacted with 2 equiv of P(1-Ad)$_2$^{n}Bu in toluene-d_8 at room temperature (eq 5).

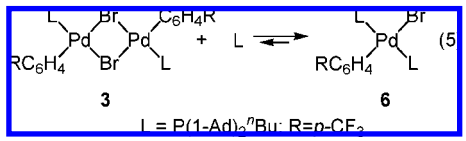

Indeed, the reaction resulted in an equilibrium mixture consisting of starting complex **3**, free phosphine ligand, and complex **6** in ca. 1:1:3.9 ratio as evidenced by ^{31}P{^{1}H} NMR spectra. Due to reversibility of the reaction, we failed to isolate complex **6**; however, it was characterized in the mixture by ^{1}H, ^{31}P{^{1}H}, and ^{13}C{^{1}H} NMR and HR-ESI mass spectra.

Unlike the bisphosphine aryl bromide complexes of P(1-Ad)$_2$^{n}Bu and P^{t}Bu$_2$^{n}Bu, the corresponding chloride complex of P^{t}Bu$_2$^{n}Bu (**7**) was successfully prepared and characterized by NMR and X-ray analysis. **7** was obtained via oxidative addition of 4-chlorobenzotrifluoride to **2** in toluene at 70 °C to give the product in 69% yield (eq 6).

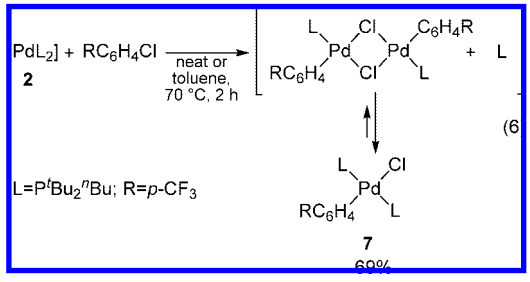

Single crystals of **7** suitable for X-ray analysis were obtained via solvent diffusion of methanol into a solution of the complex in dichloromethane at −28 °C. The molecular structure of **7** is shown in Figure 5, and selected bond lengths and angles are listed in Table 5.

Similarly to arylpalladium complexes **3** and **4**, bisphosphine complex **7** possesses an eclipsed arrangement of the aryl substituent and the *n*-butyl groups along the Pd−P bond. In solution, **6** and **7** exist in *trans* form and exhibit an equilibrium between two conformers in a ratio of 4.6:1 (−36 °C in toluene-d_8) for **6** and 6:1 (−60 °C in THF-d_8) for **7**, respectively. This is illustrated by variable-temperature ^{31}P{^{1}H} and ^{1}H NMR spectra of **7** in THF-d_8 (Figure 6). At room temperature, the ^{31}P{^{1}H} NMR spectrum of **7** contains a broad singlet at 33.2 ppm. Upon cooling of the solution to −60 °C, the peak transforms into a singlet at 29.8 ppm (major form) and two doublets at 39.3 and 31.6 ppm (minor form, $^2J_{PP}$ = 378 Hz) in a ratio of 6:1.

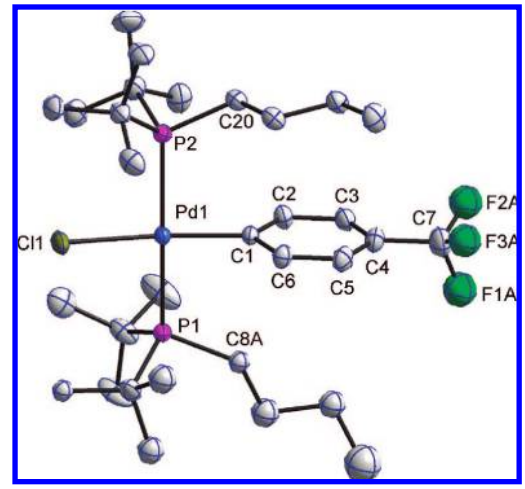

Figure 5. Molecular structure of **7**. Hydrogen atoms are omitted for clarity. The thermal ellipsoids correspond to 30% probability.

Table 5. Selected Bond Lengths (Å) and Angles (°) for **7**

Pd1−C1	1.992(4)	Cl1−Pd1−P1	91.48(4)
Pd1−P1	2.383(1)	Cl1−Pd1−P2	90.68(5)
Pd1−P2	2.384(1)	P1−Pd1−P2	170.77(5)
Pd1−Cl1	2.374(1)	C8A−P1−Pd1-C1	11.5(3)
C1−Pd1−P1	88.5(1)	C20−P2−Pd1-C1	−5.7(2)
C1−Pd1−P2	90.9(1)	α[a]	86.8(1)

[a] Angle between planes defined by P1,Cl1,P2,C1,Pd1 and C1−C6 respectively.

The equivalence of the phosphorus atoms in the major form is consistent with the solid-state structure of **7** with a symmetrical arrangement of butyl groups above and below the aryl ring. Such a conformation of the major form is again evidenced by the shielding of the aliphatic protons due to the aromatic ring current effect. At low temperature the signals of the γ-methylene groups of **7** appear at higher field with respect to neighboring methyl group (Figure 6). Additionally, the methyl groups of the *tert*-butyl substituents of the coordinated ligands exhibit a triplet at 1.52 ppm ($^3J_{PH}$ = 6.2 Hz) due to the virtual P−P coupling, which is a distinctive feature of *trans*-diphosphine complexes.[31] The minor form of **7** contains two nonequivalent phosphines, as evidenced by the presence of two doublets at 39.3 and 31.6 ppm with $^2J_{PP}$ = 378 Hz. This magnitude of P−P coupling constant is indicative of complexes with mutually *trans*-located phosphine ligands.[32] A closer inspection of the aliphatic region in the ^{1}H NMR spectrum at −60 °C revealed that the minor form shows a triplet of the methyl group of the *n*-butyl substituent at 0.90 ppm, which is close to the chemical shift of the unshielded methyl group in palladium(0) complex **2** bearing the same phosphine ligand

(31) Crabtree, R. H. *The Organometallic Chemistry of the Transition Metals*, 4th ed.; John Wiley & Sons, Inc.: New York, 2005; pp 276−279.

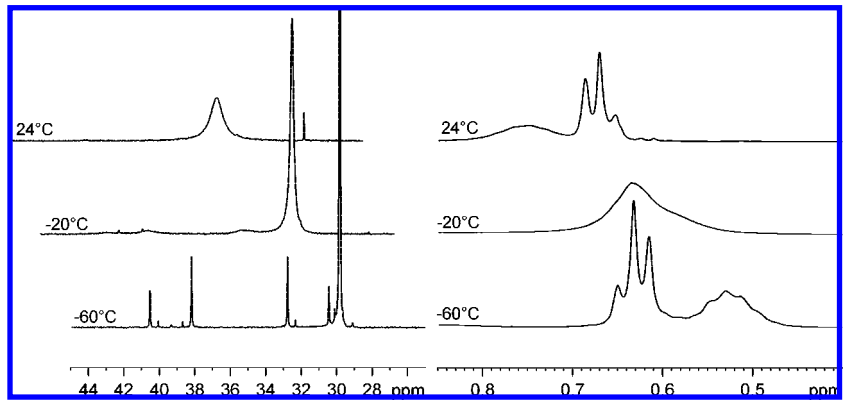

Figure 6. Variable-temperature $^{31}P\{^1H\}$ and ^1H NMR spectra of **7** in THF-d_8.

(Table 4). In contrast, the corresponding triplet of the methyl group of the major form appears at 0.63 ppm. Unshielding of the *n*-butyl protons as well as nonequivalence of phosphorus atoms in the minor form agrees with structure **7b** having two pairs of *tert*-butyl substituents in *trans* arrangement (eq 6a). Therefore, the fluxional behavior of bisphosphine complexes **6** and **7** is attributed to the equilibrium between two rotamers about the Pd−P bonds.[33]

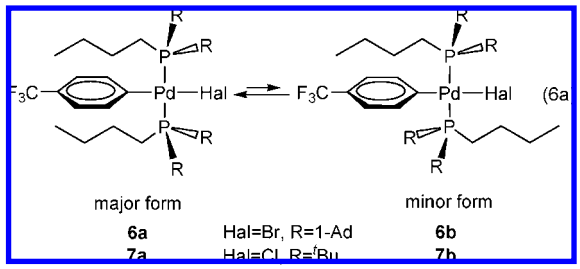

3. Synthesis, Structure, and Solution Behavior of Acylpalladium Bromide Complexes. The dimeric arylpalladium complexes **3** and **4** smoothly reacted with CO leading to dimeric acyl complexes **8** and **9** in 92 and 93% isolated yields, respectively (eq 7). Applying the same conditions, carbonylation of **5** bearing P^tBu_3 yielded the monomeric acyl complex **10** (eq 8). To the best of our knowledge, this is the first example of a three-coordinated acylpalladium complex described to date.

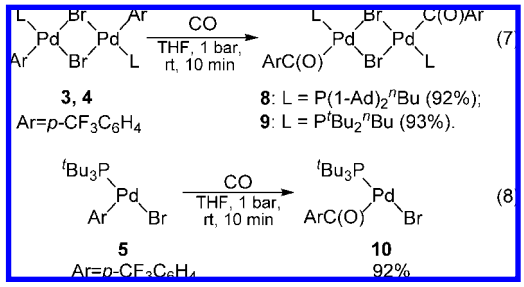

The solid-state structures of all acyl complexes were determined by X-ray crystallography, and the solution behavior of the complexes was investigated by means of ^1H, $^{31}P\{^1H\}$, and $^{13}C\{^1H\}$ NMR spectroscopy. Single crystals of **8** and **9** were grown via slow evaporation of ether and ether/dichloromethane solutions, respectively, in a vacuum at +4 °C. As shown in Figures 7 and 8, both acyl complexes exist in *trans* configuration; selected bond lengths and angles are given in Tables 6 and 7, respectively.

Each complex contains two palladium square planes bridged by the bromine atoms. The folding angle between these planes is 147.3° for **8** and 110.9° for **9**. In both complexes the acyl groups are approximately orthogonal to the respective palladium square plane and located *syn* to each other (Figure 7). In accordance with arylpalladium complexes **3**, **4**, and **7** the acyl complexes **8** and **9** contain an eclipsed arrangement of the *n*-butyl groups and the acyl substituents about the Pd−P bonds. Consequently, the methyl groups of the *n*-butyl substituents take a position above the plane of the aromatic ring.

As shown in Figure 9, the acyl complex of P^tBu_3 (**10**) possesses a distorted T-shaped geometry; see Table 8 for selected bond lengths and angles. Here, one of the hydrogen atoms (H20A) of the phosphine ligand is located close to the metal center (2.47 Å), which implies a weak agostic interaction.[34] The reason for the preference for this particular configuration can hardly be explained by steric effects, since tri-*tert*-butylphosphine occupies a position *cis* to the acyl ligand, rather than to the less bulky bromine atom.[28] However, the placement of the acyl substituent opposite to the free coordination site may be a result of the large *trans* influence. Clearly, in complex **10**, aroyl has the largest *trans* influence among all three ligands.[35] A similar configuration is known for the three-coordinate arylpalladium halide complexes of bulky phosphines[23,24] and carbene ligands.[36]

To our surprise, the coordinative unsaturated acyl complex **10** is stable in solution (THF-d_8) and does not decompose to a considerable extent within 2 days, as shown by ^1H and $^{31}P\{^1H\}$ NMR spectra. This is in contrast to the common belief that three-coordinate palladium acyl complexes readily decompose via decarbonylation reactions (eq 9).[37]

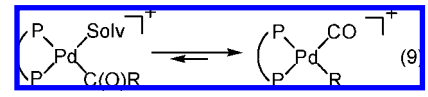

Since the acylpalladium complexes **8**−**10** are crucial species in the product-forming step of the formylation of aryl bromides, their solution behavior is especially important. Hence, we investigated the structures of **8**−**10** in detail using 1D and 2D

(32) $^2J_{PP}$ for *trans*-diphosphine palladium complexes usually exceeds 200 Hz, whereas for *cis*-ones $^2J_{PP}$ is less than 80 Hz: (a) Berger, S.; Braun, S.; Kalinowsky, H.-O. *NMR-Spectroskopie von Nichtmetallen. 31P NMR-Spectroscopie, Band 3*; Thieme; Stuttgart/New York, 1993; pp 159−160. (b) Verkade, J. G. *Coord. Chem. Rev.* **1972**, *9*, 1.

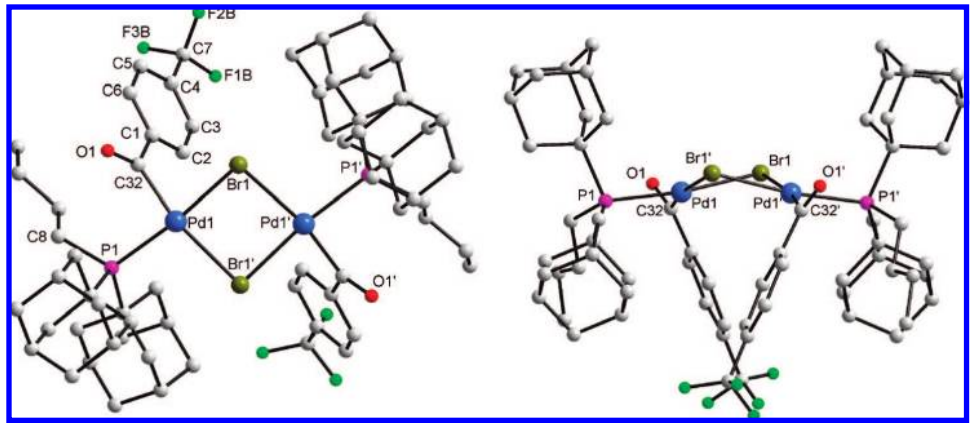

Figure 7. Molecular structure of **8**·0.3Et_2O. Hydrogen atoms are omitted for clarity. The asymmetric unit contains half of the molecule; the remaining part is generated by the following symmetry operator: $-x + 5/4$, $-y + 1/4$, $-z + 5/4$.

Table 6. Selected Bond Lengths (Å) and Angles (°) for **8**·0.3Et_2O

Pd1−C32	1.967(5)	C32−Pd1−Br1	85.0(1)
Pd1−P1	2.306(1)	P1−Pd1−Br1′	100.22(3)
Pd1−Br1	2.5254(5)	Pd1−Br1−Pd1′	89.39(2)
Pd1−Br1′	2.6048(6)	C8−P1−Pd1−C32	3.3(2)
C32−Pd1−Br1′	168.9(2)	α[a]	147.3(1)
Br1−Pd1−Br1′	84.75(2)	β[b]	77.7.(1)

[a] Folding angle between planes defined by P1,C32,Pd1,Br1,Br1′ and P1′,C32′,Pd1′,Br1,Br1′ respectively. [b] An angle between planes defined by P1,C32,Pd1,Br1,Br1′ and C32,C1−C6 respectively.

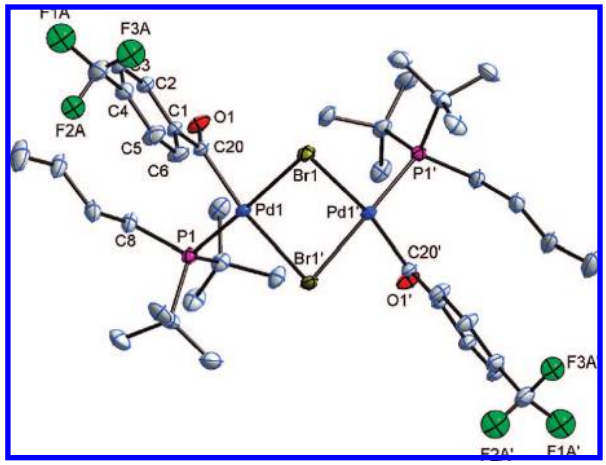

Figure 8. Molecular structure of **9**. Hydrogen atoms are omitted for clarity. The asymmetric unit contains half of the molecule; the remaining part is generated by the following symmetry operator: $-x - 1/2$, y, $-z + 3/2$. The thermal ellipsoids correspond to 30% probability.

Table 7. Selected Bond Lengths (Å) and Angles (°) for **9**

Pd1−C20	1.979(3)	C20−Pd1−Br1	85.9(1)
Pd1−P1	2.3016(9)	P1−Pd1−Br1′	100.85(3)
Pd1−Br1	2.5274(5)	Pd1−Br1−Pd1′	78.70(1)
Pd1−Br1′	2.6329(4)	C20−Pd1−P1−C8	−10.9(2)
C20−Pd1−P1	90.7(1)	α[a]	110.91(2)
Br1−Pd1−Br1′	82.87(2)	β[b]	69.59(8)

[a] Folding angle between planes defined by P1,C20,Pd1,Br1,Br1′ and P1′,C20′,Pd1′,Br1,Br1′ respectively. [b] Angle between planes defined by P1,C20,Pd1,Br1,Br1′ and C20,C1−C6 respectively.

NMR experiments. The dimeric structures of **8** and **9** in solution were confirmed by the formation of the mixed dimer **11** upon mixing **8** and **9** in THF-d_8 (eq 10).

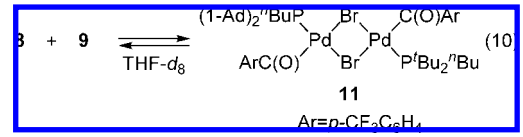

Indeed, in the $^{31}P\{^1H\}$ NMR spectrum of the mixture, two new broad singlets (52.3 and 47.8 ppm) of **11** appeared in addition to signals of the starting complexes **8** (52.9 ppm) and **9** (47.8 ppm). More specifically, **8** and **9** show a fluxional behavior which is consistent with three dynamic processes: *cis*−*trans* isomerization and hindered rotation about both Pd−P and Pd−C bonds. Since the trends observed in the temperature-dependent NMR spectra of **8** an **9** are very similar, here we discuss only the NMR behavior of **8** as an example. At room temperature the $^{31}P\{^1H\}$ NMR spectrum of **8** in THF-d_8 displays a broad singlet at 47.3 ppm. On cooling of the solution to −60 °C, this signal transforms into four singlets with a relative intensity of 85.5:9.6:3:2.8. The major singlet at 47.0 ppm is assigned to the *trans* form of the complex. Other minor signals are attributed to various conformers of *trans* and *cis* isomers. Analysis of the variable-temperature ^1H NMR spectra of **8** shows that, in contrast to the corresponding aryl complex **3**, the acyl complex **8** exhibits hindered rotation about the Pd−C bond, which results in nonequivalence of four aromatic protons at −100 °C (Figure 10).

More specifically, at room temperature, rotation of the *p*-trifluoromethylbenzoyl group is fast on the ^1H NMR time scale, and **8** displays two doublets at 7.76 and 8.46 ppm, corresponding to protons in positions *ortho* to the CF_3 (H3, H5) and C(O) groups (H2, H6), respectively (Figure 11). However, when the temperature is decreased to −20 °C, the doublet of aromatic protons adjacent to the carbonyl group (H2, H6) turns into a broad singlet, whereas the doublet of protons H3, H5 broadens only slightly. Clearly, protons H2 and H6 are closer to the sterically congested palladium atom compared to protons H3 and H5. Therefore, slowing down the rotation of the acyl group has a more pronounced influence on the chemical shifts of H2 and H6. At −60°, two broad singlets at 7.87 and 9.41 ppm are observed, which at −100 °C transform into four broadened doublets at 7.59, 7.76, 8.11, and 9.43 ppm corresponding to the major *trans* form of **8**. Additionally, a small broad doublet at 9.65 ppm corresponds to one of the minor isomers, which is in ca. 1:10 ratio to the major form. Considering the proton spectra of the *trans* form, one can see that the doublet

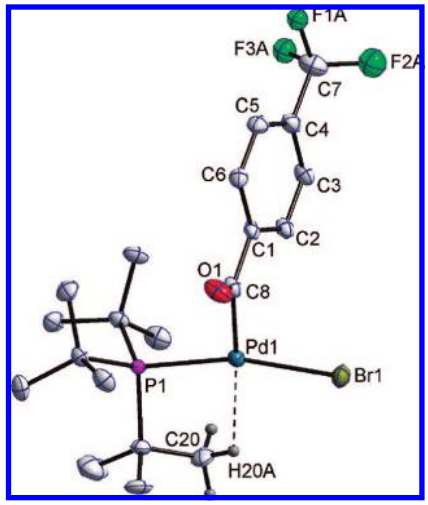

Figure 9. Molecular structure of **10**. Hydrogen atoms (except those attached to C20) are omitted for clarity. The thermal ellipsoids correspond to 30% probability.

Table 8. Selected Bond Lengths (Å) and Angles (°) for **10**

Pd1−C8	1.946(4)	O1−C8−C1−C6	−16.9(6)
Pd1−P1	2.3069(10)	C8−Pd1−Br1	93.0(1)
Pd1−Br1	2.4484(5)	P1−Pd1−Br1	165.19(3)
C8−Pd1−P1	101.1(1)	α[a]	74.8(1)

[a] Angle between planes defined by P1,Pd1,Br1,C8 and C1−C6,C8 respectively.

at 9.43 ppm exhibits a significant low-field shift comparing to the other three doublets of the trifluoromethylbenzoyl group. This low-field doublet is assigned to proton H2 located above the coordination plane in close proximity to the metal center (Figure 11). The pronounced deshielding of this proton is due to the paramagnetic anisotropy of the palladium atom.[38]

Similar to the aryl complexes, the acyl complexes **8** and **9** show a comparable arrangement of the *n*-butyl moiety of the phosphine ligand, lying over the aromatic ring of the acyl group, as evidenced by the shielding of *n*-butyl protons. The methyl and γ-methylene protons of the *n*-butyl groups are located close to the centers of the aromatic rings and display a pronounced downfield chemical shift as compared to the corresponding protons of the phosphine ligand in palladium(0) complexes **1** and **2**. For example, at −100 °C the γ-methylene and methyl protons of the *n*-butyl group of **8** are shifted by 0.86 and 0.83 ppm toward high field with respect to the corresponding signals of **1**. Notably, the monomeric acyl complex **10** does not exhibit a dynamic behavior in the ^{1}H and ^{31}P{^{1}H} NMR spectra at room temperature.

Next, we studied the reactivity of **8**−**10** in the presence of additional phosphines because, under catalytic conditions, an excess of ligand is used. Interestingly, according to the NMR spectra, the three-coordinate complex **10** did not react with excess of the tri-*tert*-butylphosphine.[39] Addition of 2 equiv of the phosphine did not lead to the formation of any new signals in the ^{1}H and ^{31}P{^{1}H} NMR or broadening of existing ones.[40] In contrast, **8** and **9** react reversibly with the phosphine ligands to give an equilibrium mixture of the corresponding *trans*-bisphosphine acyl complexes **12** and **13** (eq 11).

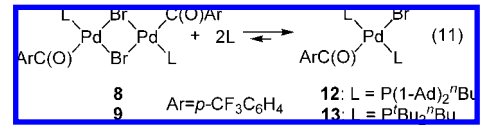

Thus, addition of 2 equiv of P(1-Ad)$_2{}^n$Bu to complex **8** led to an equilibrium mixture of the starting dimer **8** and the bisphosphine complex **12** in a 1:2.2 ratio. When the temperature decreases, the equilibrium shifts toward **12**, implying that the

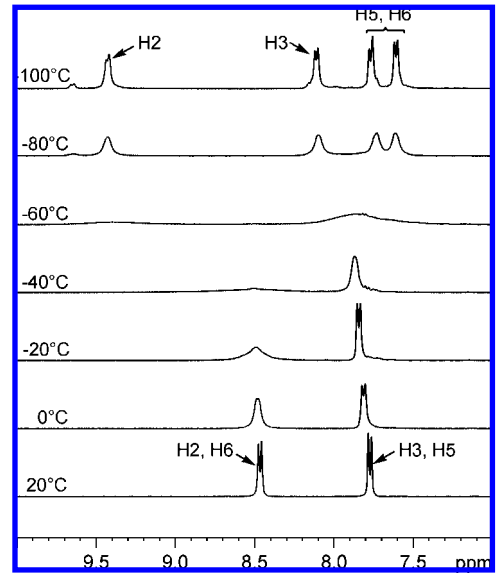

Figure 10. Variable-temperature ^{1}H NMR spectrum of **8** in THF-d_8. The assignment of the aromatic protons at −100 °C is confirmed by COSY and HMQC.

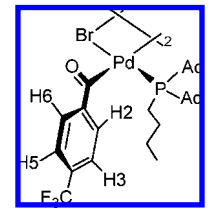

Figure 11. Orientation of the trifluoromethylbenzoyl moiety in **8**. Numbering of aromatic protons corresponds to the crystal structure of **8**.

(33) Analogous rotamers were reported for other square-planar *trans* complexes with similar phosphine ligands, *trans*-[Pd(Hal)$_2$(P^{t}Bu$_2$H)$_2$], *trans*-[Pd(Hal)(CO)(P^{t}Bu$_2$H)$_2$], and *trans*-[M(Cl)(CO)(P^{t}Bu$_2$R)$_2$] (M = Ir, Rh): (a) Mann, B. E.; Masters, C.; Shaw, B. L.; Stainbank, R. E. *J. Chem. Soc. D* **1971**, 1103. (b) Bright, A.; Mann, B. E.; Masters, C.; Shaw, B. L.; Slade, R. M.; Stainbank, R. E. *J. Chem. Soc. A* **1971**, 1826.

(34) Sum of van der Waals radii of palladium and hydrogen is 2.8 Å: Bondi, A. *J. Phys. Chem.* **1964**, *68*, 441. Some reviews on agnostic interaction: (a) Brookhart, M.; Green, M. L. H. *J. Organomet. Chem.* **1983**, *250*, 395. (b) Brookhart, M.; Green, M. L. H.; Wong, L.-L. *Prog. Inorg. Chem.* **1988**, *36*, 1.

(35) Appleton, T. G.; Clark, H. C.; Manzer, L. E. *Coord. Chem. Rev.* **1973**, *10*, 335.

(36) Computational calculations of all possible isomers of [Pd(I^{t}Bu)(Ph)(Cl)] showed that the most stable configuration is that with phenyl *trans* to the free position: Green, J. C.; Herbert, B. J.; Lonsdale, R. *J. Organomet. Chem.* **2005**, *690*, 6054.

(37) (a) Tóth, I.; Elsevier, C. J. *J. Am. Chem. Soc.* **1993**, *115*, 10388. (b) Shultz, C. S.; Ledford, J.; DeSimone, J. M.; Brookhart, M. *J. Am. Chem. Soc.* **2000**, *122*, 6351. (c) Ledford, J.; Shultz, C. S.; Gates, D. P.; White, P. S.; DeSimone, J. M.; Brookhart, M. *Organometallics* **2001**, *20*, 5266. (d) Bianchini, C.; Meli, A.; Müller, G.; Oberhauser, W.; Passaglia, E. *Organometallics* **2002**, *21*, 4965.

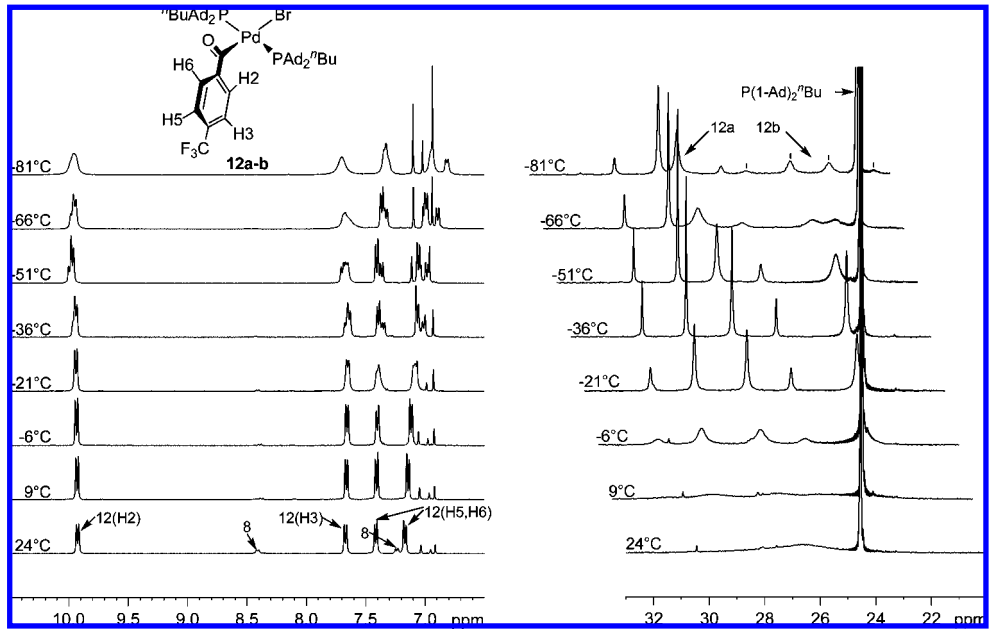

Figure 12. Variable-temperature ^{1}H and ^{31}P{^{1}H} NMR spectra of **12** formed by mixing **8** with P(1-Ad)$_2$^{n}Bu (5 equiv) in toluene-d_8. The assignment of the aromatic protons was confirmed by COSY.

reaction is exothermic. Thus, by lowering the temperature from +9 to −51 °C, the ratio of **8** to **12** is increased from 1:8.7 to 1:100.

Both complexes **12** and **13** exist in solution as two conformers due to the hindered rotation about the Pd−P bonds. This is illustrated by variable-temperature NMR spectra of **12** in toluene-d_8 (Figure 12). At room temperature, both conformers are in fast equilibrium on the ^{1}H NMR time scale. However, in contrast to **8**, both conformers of **12** exhibit a restricted rotation about the Pd−C bond already at room temperature. This is evidenced in the ^{1}H NMR spectrum by the presence of four broadened doublets at 9.98, 7.73, 7.47, and 7.23 ppm, corresponding to the four nonequivalent aromatic protons of the *p*-trifluoromethylbenzoyl group (Figure 12).

In **12** the aroyl group is orthogonal to the palladium square plane. As a result, the appearance of a low-field doublet at 9.98 ppm is indicative of the aromatic proton H2 directed toward the palladium center. Upon cooling of the solution to −51 °C, the set of four doublets splits into two groups of doublets at 9.97, 7.66, 7.40, 7.05 ppm and 9.99, 7.69, 7.36, 6.98 ppm, corresponding to a pair of conformers in ca. 2.2:1 ratio. In the ^{31}P{^{1}H} NMR spectrum, *major* and *minor* conformers display two doublets at 29.6 and 26.3 ppm ($^2J_{PP}$ = 256 Hz) and one broadened singlet at 23.0 ppm, respectively (see Figure 12). Whereas the *major* form displays two doublets in the temperature range starting from the coalescence point to −81 °C, the singlet of the *minor* form at 23 ppm transforms into two broad doublets at 24.4 and 21.4 ppm ($^2J_{PP}$ = 260 Hz) when the temperature decreases below −51 °C. *Major* and *minor* conformers have $^2J_{PP}$ constants exceeding 200 Hz, which allows for an unambiguous assignment of the *trans* configuration to both species. Finally, we suppose that the dynamic behavior of **12** is explained by an equilibrium between the two rotamers depicted in Figure 13. The major form is assigned to rotamer **12a**, whereas the minor species corresponds to two degenerated rotamers **12b**.

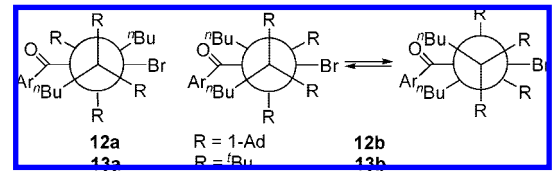

Figure 13. Newman projections of two rotamers of complexes **12** and **13** along the P−Pd−P direction.

In addition, when the temperature decreases to −66 °C, one of the two doublets of **12a** at 26.3 ppm broadens to a much greater extent that the second one. This is attributed to a hindered rotation of one of the sterically encumbered adamantyl groups about the P−C bond. As shown in the Newman projection of **12a** (Figure 13), one adamantyl group bound to the rear phosphorus atom is "clutched" between the oxygen atom of the acyl substituent and another adamantyl group. Complex **13** shows a similar dynamic behavior, except that the coalescence temperature in ^{31}P{^{1}H} NMR for the equilibrium between **13a** and **13b** is lower (0 °C) and the two degenerated rotamers **13b**

(38) (a) Miller, R. G.; Stauffer, R. D.; Fahey, D. R.; Parnell, D. R. *J. Am. Chem. Soc.* **1970**, *92*, 1511. (b) Deeming, A. J.; Rothwell, I. P.; Hursthouse, M. B.; New, L. *J. Chem. Soc., Dalton Trans.* **1978**, 1490. (c) Widenhoefer, R. A.; Zhong, H. A.; Buchwald, S. L. *Organometallics* **1996**, *15*, 2745. (d) Albert, J.; Cadena, J. M.; Granell, J. R.; Solans, X.; Font-Barida, M. *Tetrahedron Asymmetry* **2000**, *11*, 1943. (e) Barloy, L.; Gauvin, R. M.; Osborn, J. A.; Sizun, C.; Graff, R.; Kyritsakas, N. *Eur. J. Inorg. Chem.* **2001**, 1699. (f) Riera, X.; Moreno, V.; Feisinger, E.; Lippert, B. *Inorg, Chim. Acta* **2002**, *339*, 253.

(39) Similarly, Hartwig et al. did not observe any reaction of the three coordinate aryl complex [Pd(Br)(Ph){P(1-Ad)^{t}Bu$_2$}] with added P(1-Ad)^{t}Bu$_2$, see ref 23.

(40) In contrast, complex **10** reacts with 1 equiv of P(1-Ad)$_2$^{n}Bu at room temperature in toluene-d_8 yielding the acyl complex **8** and free P^{t}Bu$_3$ in quantitative yield. This result illustrates (1) the possibility of phosphine exchange processes in **10**, which could proceed via four coordinate bisphosphine intermediates, and (2) stronger binding of P(1-Ad)$_2$^{n}Bu to palladium(II) as compared to P^{t}Bu$_3$.

(41) A similar decelerating effect of phosphine additives was observed in the hydrogenolysis of cobalt and ruthenium acyl complexes that proceeds via formation of coordinatively unsaturated species. See for example: Joshi, A. M.; James, B. R. *Organometallics* **1990**, *9*, 199, and references therein.

are in fast exchange, even at −80 °C, which is in agreement with the lower steric bulk of *tert*-butyl groups as compared to adamantyl ones.

4. Synthesis and Structure of Palladium Hydride Complexes. Palladium hydride complexes are assumed to result from the hydrogenation of the acyl complexes.[15] Hence, we synthesized novel palladium hydrobromide complexes having di-1-adamantylalkylphosphine (**14**) and di-*tert*-butylalkylphosphine (**15**) ligands. They were smoothly prepared by addition of pyridine hydrobromide in acetonitrile to a toluene solution of the corresponding [PdL_2] complexes at room temperature (eq 12).

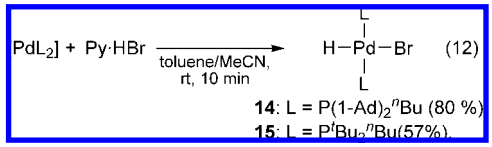

Single crystals of **14** suitable for X-ray analysis were obtained by diffusion of ether into a solution of **14** in dichloromethane at room temperature. The structure of **14** is depicted in Figure 14. Selected bond lengths and angles are given in Table 9.

Complex **14** exhibits a *gauche* conformation of the substituents. The P1−Pd−P2 angle of 166.9° is appreciably distorted from the linear one. Interestingly, the angle is bent in a direction that brings two *gauche*-adamantyl groups close to each other. This geometry may be explained by minimization of steric repulsion between the bulky adamantyl substituents and the bromine atom. As a result, the hydrogen atom is effectively shrouded by two adamantyl groups.

5. Hydrogenolysis of Acylpalladium Complexes with Synthesis Gas. Notably, all performed stoichiometric transformations of the palladium complexes bearing either P(1-Ad)$_2$^{n}Bu, P^{t}Bu$_2$^{n}Bu, or P^{t}Bu$_3$ up to the corresponding acyl complexes proceeded with high yields whatever the ligand used. However, product yields and efficiency of the catalytic reactions utilizing ligands P(1-Ad)$_2$^{n}Bu and P^{t}Bu$_2$^{n}Bu on the one hand and P^{t}Bu$_3$ on the other hand differed drastically. Intrigued by this pronounced discrepancy, we studied the hydrogenation of the different acylpalladium complexes, which is the product-forming step of the formylation of aryl bromides. As a starting point we chose the hydrogenation of **8** at 5 bar of synthesis gas in toluene-d_8 (eq 13). Here, we examined the influence of phosphine ligands, base, and temperature on the reaction course (Table 10).

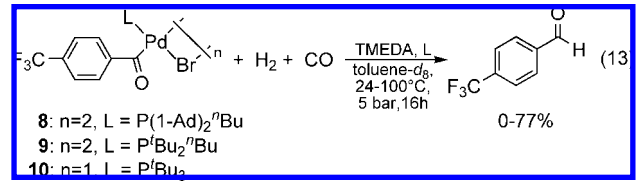

The reaction mixtures were analyzed by ^{1}H and ^{31}P{^{1}H} NMR; conversions and yields were measured using 1,4-dimethoxybenzene as an internal standard for ^{1}H NMR. At 50 °C, hydrogenolysis of **8** did not proceed without additives, and the starting complex precipitated from the reaction mixture (Table 10, entry 4). Interestingly, addition of 4 equiv of TMEDA dramatically accelerated the desired reaction, yielding 4-trifluoromethylbenzaldehyde in 76% yield at full conversion (Table 10, entry 6). A similar result was obtained in the presence of a 100-fold excess of TMEDA (Table 10, entry 7). Under the same conditions, the P^{t}Bu$_2$^{n}Bu ligated complex **9** gave the aldehyde in 74% yield (Table 10, entry 10). In the presence of base, hydrogenation of **8** can be effected even at room temperature (Table 10, entry 2). An increase in the concentration of the base improves both the yield and the conversion (Table 10, entries 1−3), while an increase in phosphine concentration hampers the reaction and decreases the aldehyde yield to 54% (Table 10, entries 6, 8−9). The decelerating effect of phosphine is consistent with the formation of coordinatively unsaturated species prior to hydrogenolysis of the Pd−C_{acyl} bond.[41] In this respect the activation effect of the amine seems rather unusual, since TMEDA is also prone to bidentate coordination, thus blocking free coordination sites. In order to clarify if the activation effect of TMEDA is due to its reaction with the acyl complex, we compared the ^{1}H and ^{31}P{^{1}H} NMR spectra of the dimeric acyl complex **8** in toluene-d_8 in the presence and in the absence of a 4-fold molar excess of TMEDA. However, the ^{1}H and ^{31}P{^{1}H} NMR spectra did not reveal any appreciable differences.[42]

To rationalize the accelerating effect of the base, the possible pathways for hydrogenolysis of acyl complexes are shown in Figure 15. In agreement with known mechanisms,[43,44] we suppose that, prior to hydrogenolysis, the dimeric acyl complexes **8** and **9** dissociate to give coordinatively unsaturated

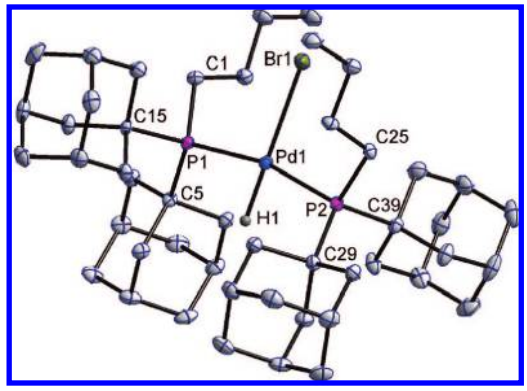

Figure 14. Molecular structure of **14**. The asymmetric unit contains two molecules with similar bond lengths and angles; therefore, only one molecule is depicted. All hydrogen atoms except H1 are omitted for clarity. The thermal ellipsoids correspond to 30% probability.

Table 9. Selected Bond Lengths (Å) and Angles (°) for **14**

Pd1−P1	2.3096(7)	C15−P1−Pd1−Br1	−90.6(1)
Pd1−P2	2.3082(7)	C39−P2−Pd1−Br1	−90.1(1)
Pd1−Br1	2.5448(5)	C5−P1−Pd1−Br1	144.0(1)
P1−Pd1−P2	166.89(3)	C29−P2−Pd1−Br1	142.7(1)
P1−Pd1−Br1	96.12(2)	C15−P1−P2−C39	174.9(1)
P2−Pd1−Br1	96.99(2)	C1−P1−P2−C29	169.2(2)
C1−P1−Pd1−Br1	23.7(1)	C1−P1−P2−C25	49.4(2)
C25−P2−Pd1−Br1	23.2(1)	C5−P1−P2−C29	−70.2(1)

(42) In contrast, NMR spectra of the mixture in THF-d_8 at room temperature display a rather complicated picture including equilibrium between starting complex **8** and at least four new species. ^{31}P{^{1}H} NMR spectrum recorded at−40°C showed the presence of four major groups of multiplets: two doublets at 26.5 and 29.9 ppm ($^2J_{PP}$ = 256 Hz) and at 27.1 and 30.8 ppm ($^2J_{PP}$ = 265 Hz) and two broad singlets at 23.8 and 22.7 ppm in ca. 3:1.3:1.3:1 ratio.

(43) Stanley, G. G. In *Comprehensive Organometallic Chemistry III*; Mingos, D. M., Crabtree, R. H., Canty, A., Eds.; Elsevier: Oxford, 2007; Vol. 1, pp 119−140.

(44) Jessop, P. G.; Morris, R. H. *Coord. Chem. Rev.* **1992**, *121*, 155.

(45) In contrast to many other transition metals, palladium does not form η^2-dihydrogen complexes sufficiently stable to be detected at room temperature, but their existence was supported by theoretical calculations: Kubas, G. *J. Organomet. Chem.* **2001**, *635*, 37, and references therein.

Table 10. Hydrogenolysis of Acylpalladium Complexes **8**−**10**[a]

entry	complex	*T* (°C)	TMEDA (equiv)	ligand (equiv)	conversion (%)	yield ArCHO (%)	main organometallic products
1	**8**	24	0	0	0	0	−
2	**8**	24	4	0	79	34	nd
3	**8**	24	20	0	97	56	**17**, **14** (13.2:1)[b]
4	**8**	50	0	0	0	0	−
5	**8**	50	0	4	11	0	nd
6	**8**	50	4	0	100	76	**17**
7	**8**	50	100	0	100	77	**17**
8	**8**	50	4	4	100	73	**17**, **14** (4:1)[b]
9	**8**	50	4	12	83	54	**17**, **14** (1:1.3)[b]
10	**9**	50	100	0	100	74	nd
11	**10**	50	0	0	31	17	nd
12	**10**	50	2	0	100	0	**16** (precipitate)
13	**10**	50	0	2	28	11	nd
14	**8**	100	0	0	100	25	**14**+ Pd black
15	**8**	100	4	0	100	43	Pd black + $P(1\text{-Ad})_2{}^n$Bu
16	**8**	100	20	0	100	62	Pd black + $P(1\text{-Ad})_2{}^n$Bu
17	**8**	100	100	0	100	73	Pd black + $P(1\text{-Ad})_2{}^n$Bu
18	**8**	100	0	4	100	61	**14** + Pd black
19	**8**	100	4	4	100	67	**14** + Pd black
20	**8**	100	4	8	100	70	**14** + Pd black
21	**9**	100	0	0	100	28	nd
22	**9**	100	4	0	100	67	Pd black + $P^tBu_2{}^n$Bu
23	**9**	100	0	4	100	68	**15**+ Pd black
24	**9**	100	4	4	100	74	**15**+ Pd black
25	**10**	100	0	2	100	57	Pd black + P^tBu_3
26	**10**	100	2	0	100	52	Pd black + P^tBu_3

[a] Reaction conditions: 5 bar of CO/H_2 (1:1), toluene-d_8, 100 °C, 16 h. Conversions and yields were measured by ^{1}H NMR spectra using 1,4-dimethoxybenzene as internal standard. [b] The ratio of the signals in the $^{31}P\{^1H\}$ NMR spectra.

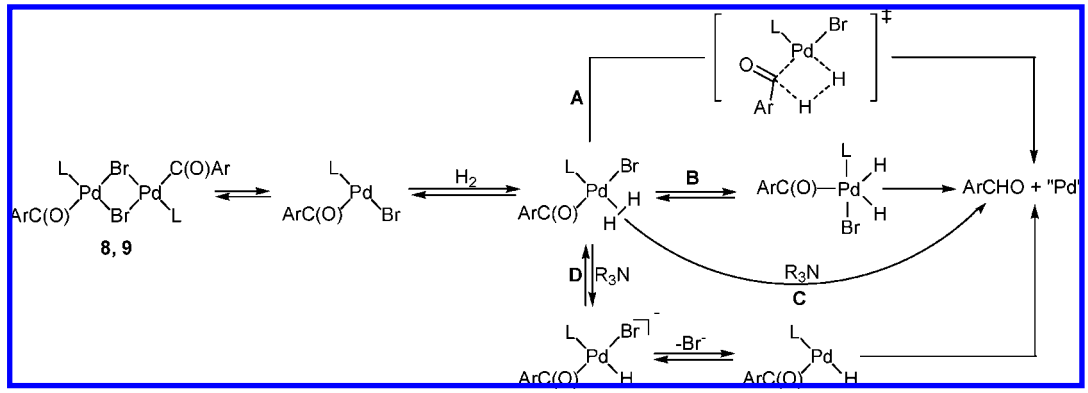

Figure 15. Possible pathways for the hydrogenolysis of acylpalladium bromide complexes **8** and **9**.

monomers that reversibly react with hydrogen, resulting in η^2-dihydrogen complexes.[45] These complexes can give rise to the aldehyde via four different pathways. Pathway A includes direct σ-metathesis of H−H and Pd−C bonds, furnishing the aldehyde in one step. Pathway B consists of formation of an intermediate dihydride Pd(IV) species,[46] followed by reductive elimination of aldehyde. Moreover, the η^2-dihydrogen complex might undergo a base-assisted heterolytic cleavage of the coordinated dihydrogen to give the aldehyde directly (pathway C) or via formation of an anionic intermediate (pathway D).

Clearly, pathway A is not consistent with the participation of the base. Pathway B includes formation of highly unstable dihydrido spices of palladium(IV) that should rapidly undergo reductive elimination; therefore, it is unlikely that base can mediate this process. In contrast, pathways C and D, including heterolytic cleavage of the coordinated dihydrogen, agree with the accelerating role of the base. It is well known that η^2-coordinated dihydrogen has increased acidity. For example, η^2-dihydrogen ruthenium complexes are deprotonated even with mild bases, resulting in the corresponding monohydride complexes.[47] This process is believed to be involved in base-mediated ruthenium-catalyzed hydrogenation.[48] In addition, intramolecular heterolytic cleavage of η^2-dihydrogen was proposed as a plausible pathway for the hydrogenolysis of acyl carboxylato palladium complexes. However, this pathway is difficult to distinguish from A and B.[49] So far, to the best of

(46) It is known that η^2-dihydrogen complexes are often in equilibrium with their dihydrido tautomers. For more information, see ref 47.

(47) (a) Tye, J. W.; Hall, M. B. In *Activation of Small Molecules. Organometallic and Bioinorganic Perspectives*; Tolman, W. B., Ed.; Wiley-VCH: Weinheim, 2006; pp 121−150. (b) Henderson, R. A. *Transition Met. Chem.* **1988**, *13*, 474. (c) Esturelas, M. A.; Oro, L. A. *Chem. Rev.* **1998**, *98*, 577. (d) Kubas, G. J. *Metal Dihydrogen and σ-bond Complexes*; Kluwer Academic: New York, 2001; pp 268−295.

(48) See for example: (a) Kitamura, M,; Noyori, R. In *Ruthenium in Organic Synthesis*; Murahashi, S.-I., Ed.; Wiley-VCH: Weinheim, 2004; pp 3−52. (b) Stanley, G. G. In *Comprehensive Organometallic Chemistry III*; Mingos, D. M., Crabtree, R. H., Parkin, G., Eds.; Elsevier: Oxford, 2007; Vol. 1, pp 119−163.

our knowledge, no base-assisted intermolecular heterolytic cleavage of dihydrogen is reported for palladium acyl complexes nor for the corresponding complexes of any other transition metal. In view of this, the base-mediated hydrogenation of complexes **8** and **9** seems rather remarkable.

In contrast to **8** and **9**, the P^{t}Bu$_3$-ligated acyl complex **10** is completely inactive under similar conditions (toluene, TMEDA, 5 bar of synthesis gas, 50 °C; Table 10, entry 12). Under these conditions, **10** formed the diamino complex **16** via displacement of P^{t}Bu$_3$ (eq 14). In a separate experiment we showed that addition of 2 equiv of TMEDA to a toluene solution of **10** led to a precipitate of pale yellow crystals of **16** in 98% yield. A similar substitution of P^{t}Bu$_3$ in arylpalladium complexes [Pd(Ar)(Br)(P^{t}Bu$_3$)] was observed by Hartwig and co-workers.[50]

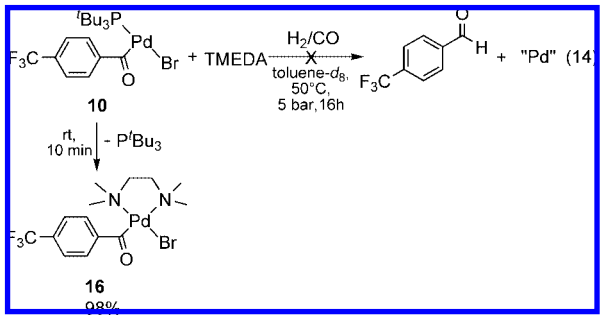

The obtained data for the stoichiometric hydrogenolysis experiments of acyl complexes **8** and **10** are in good agreement with results of the catalytic formylation (eq 1). Indeed, poor activity of the Pd/P^{t}Bu$_3$ system is explained by the formation of the insoluble diamino complex **16**. In contrast, P(1-Ad)$_2$^{n}Bu, P^{t}Bu$_2$^{n}Bu ligated complexes **8** and **9** are stable toward the amine. Hence, they operate under catalytic reaction conditions, where 300-fold excess of the base is used. Furthermore, an increase in base concentration promotes the hydrogenolysis. The smooth hydrogenolysis of complexes **8** and **9** explains the rather low pressure of synthesis gas (5 bar) needed for the catalytic formylation in the presence of Pd/P(1-Ad)$_2$^{n}Bu. For comparison, the previously reported catalyst based on [Pd(PPh$_3$)Cl$_2$] enabled formylation of bromobenzene with synthesis gas at 93 bar at 150 °C,[5] which is in agreement with the high pressure of hydrogen (60 bar at 60 °C) needed for hydrogenolysis of *trans*-[Pd(Br){C(O)Ph}(PPh$_3$)$_2$].[15]

To compare the reactivity of the acyl complexes under reaction conditions, we further studied hydrogenation of **8**−**10** at 100 °C (Table 10, entries 14−26). At 100 °C acyl complexes **8** and **9** undergo hydrogenolysis in the absence of any additives to give the aldehyde in low yields of 25−28% (Table 10, entries 14 and 21).[51] However, addition of TMEDA led to a significant increase in the aldehyde yield (Table 10, entries 14−17, 21−22). In general, at 100 °C the product yields are somewhat lower compared to those at 50 °C (Table 10, entries 6−8 and 15, 17, 19), probably due to concurrent decomposition of the starting complex. Indeed, addition of 4 equiv of phosphine ligand, which stabilizes the catalyst system, considerably improved the yields (Table 10, entries 14 and 18−20, 21, 23). Finally, the best yields for hydrogenolysis of complexes **8** and **9** are obtained by using a TMEDA/Pd ratio of 100:1 (close to the real catalytic reaction) and a combination of TMEDA and phosphine ligand (Table 10, entries 17, 20, and 24).

To our surprise, at 100 °C the less reactive P^{t}Bu$_3$-ligated acyl complex **10** also became prone to hydrogenolysis and gave 4-trifluoromethylbenzaldehyde in moderate yields (52−57%; Table 10, entries 25−26). Moreover, in the presence of 2 equiv of phosphine or TMEDA the product yields are similar (57 and 52%), suggesting that formation of the catalytically inactive complex **16** is reversible at 100 °C (eq 14). The discrepancy between stoichiometric hydrogenation (52−57%) and catalytic formylation (4%) is explained by the larger ratio of TMEDA to palladium (300:1) used in the catalytic reaction. Apparently, the reversible formation of the active complex **10** is efficiently blocked under catalytic conditions. Indeed, close inspection of a catalytic formylation in the presence of 1 mol % of [Pd(P^{t}Bu$_3$)$_2$] after 1.5 h revealed formation of a precipitate of **16** and P^{t}Bu$_3$ as the only phosphorus-containing compound in solution.

6. The Fate of Palladium Species after Hydrogenolysis: Regeneration of Palladium(0) Species and Catalyst Stability. Hydrogenolysis of the acylpalladium complex **8** in the presence of TMEDA gave the carbonyl complex **17** as the sole palladium-containing product, displaying a singlet at 46.6 ppm in the ^{31}P{^{1}H} NMR spectrum of the reaction mixture (eq 15).

The same carbonyl species formed quantitatively when palladium(0) complex **1** was reacted with CO in toluene at room temperature (eq 16). This carbonylation proceeded rapidly with liberation of 1 equiv of phosphine ligand. Heating of the same reaction mixture in the absence of CO atmosphere gave the starting [PdL$_2$] complex, indicating the reversibility of this reaction (eq 16).

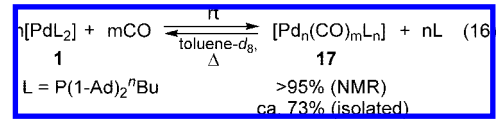

Complex **17** was isolated from the reaction mixture by precipitation with heptane in 73% yield. Although we failed to obtain single crystals suitable for X-ray analysis, **17** was characterized by IR and ^{1}H, ^{31}P{^{1}H}, and ^{13}C{^{1}H} NMR spectra. **17** contains one type of coordinated phosphine ligand, as evidenced by a singlet at 46.6 ppm in the ^{31}P{^{1}H} NMR spectrum. The presence of a bridged CO group is indicated by a strong band at 1806 cm^{-1} in the IR-ATR spectrum[52] and a broad singlet at δ 241 ppm in the ^{13}C{^{1}H} NMR.[53] These data clearly suggest a multinuclear cluster structure.[54] Carbonyl complex **17** is thermally unstable and completely decomposes to give palladium black and free ligand when heated under catalytic reaction conditions. Since palladium(0) complex **1**

(49) Yamamoto, A.; Kayaki, Y.; Nagayama, K.; Shimizu, I. *Synlett* **2000**, 925.
(50) Shen, Q.; Shekhar, S.; Stambuli, J. P.; Hartwig, J. F. *Angew. Chem., Int. Ed.* **2004**, *44*, 1371.
(51) This shows that at 100 °C hydrogenolysis of complexes **8** and **9** can partially proceed via base-free pathways A and B.
(52) Most carbonyl complexes having bridge carbonyls exhibit a ν(CO) band at 1800−1900 cm^{-1}: Nakamoto, K. *Infrared and Raman Spectra of Inorganic and Coordination Compounds*; Wiley-Interscience: New York, 1986; pp 291−301.
(53) The complex exhibits dynamic behavior in the ^{13}C{^{1}H} NMR spectrum. Detailed investigation of solution structure of this complex was not performed.

rapidly transforms into **17** in CO atmosphere, the stability of **1** under the reaction conditions is the same as that of **17**. Therefore, it is not surprising that hydrogenation of complexes **8** and **9** carried out in the presence of TMEDA at 100 °C yielded palladium black and free phosphine. The same result was obtained for complex **10** when the reaction was carried out in the presence of 2 equiv of TMEDA or P^tBu_3 (eq 17).

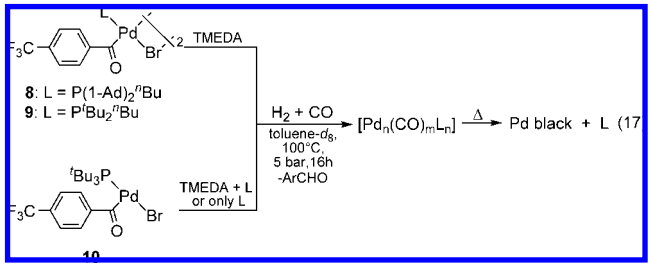

A completely different reaction pattern was observed when the hydrogenation of acyl complexes **8** and **9** was effected in the presence of additional phosphine and TMEDA (catalytic conditions). Here, the corresponding hydride complexes **14** and **15** are formed as main products. This suggests that hydride species **14** and **15**, unlike the respective carbonyl clusters, are stable at 100 °C for 16 h under synthesis gas. Moreover, it is rather surprising that these complexes were observed even when an excess of base was used (eq 18)!

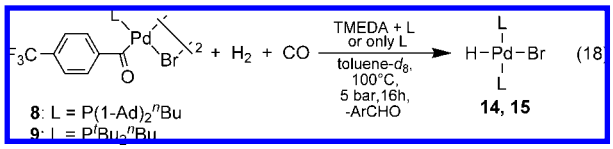

Intrigued by these results, we examined the reactivity of hydrido palladium complexes [Pd(H)(Br)L_2], L= P(1-Ad)$_2{}^n$Bu (**14**), $P^tBu_2{}^n$Bu (**15**), and P^tBu_3 (**18**), toward TMEDA in detail. When **14** or **15** was mixed with a 2-fold excess of TMEDA in toluene-d_8 at room temperature, the ^{1}H and $^{31}P\{^1H\}$ NMR spectra showed no appreciable reaction. Moreover, neither heating of **14** with 2 equiv of TMEDA at 100 °C nor use of a 100-fold excess (!) of base at room temperature showed any formation of palladium(0) complex **1** in the $^{31}P\{^1H\}$ NMR spectra (eq 19).

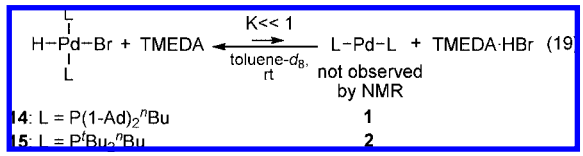

In contrast to **14** and **15**, the reaction of the P^tBu_3-ligated hydrido palladium complex **18** with TMEDA proceeded smoothly within 10 min at room temperature to give the respective palladium(0) complex quantitatively (eq 20).

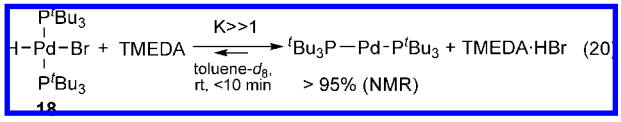

The same result was obtained when the reactions depicted in esq 19 and 20 were effected from opposite directions. For example, heating of **1** with TMEDA·HBr in toluene-d_8 at 70 °C[55] gave the hydrido complex **14** in 93% yield (eq 19). On the other hand, the reaction of [Pd(P^tBu_3)$_2$] with TMEDA·HBr in toluene-d_8 at 70 °C did not proceed to any extent (eq 20). These results imply that the reactivity of these hydrido complexes toward the base is governed by thermodynamics, but not kinetics. Therefore, the reason for the pronounced difference in the reactivity between **14**, **15**, and **18** may be revealed by comparison of the ground states of the [PdL$_2$] and [Pd(Br)(H)L$_2$] complexes. It is evident that P^tBu_3 is more sterically demanding than $P^tBu_2{}^n$Bu, and probably P(1-Ad)$_2{}^n$Bu. Since the hydridobromide complexes are more sterically encumbered as compared to the corresponding bisphosphine palladium(0) complexes, the increased steric bulk of P^tBu_3 facilitates reductive elimination from **18**. In addition, the divergent reactivity may be caused by the different electron-donating properties of the phosphines. Clearly, electron-rich phosphines stabilize a hydrido palladium(II) complex and increase the basicity of the respective palladium(0) complex, thus making dehydrobromination less favorable. To evaluate the σ-donor ability of the phosphines, we compared phosphorus−selenium ($^1J_{PSe}$) coupling constants of the corresponding phosphine selenides. The magnitude of $^1J_{PSe}$ is known to increase with decrease in basicity of the phosphine.[56] We prepared selenides of $P^tBu_2{}^n$Bu and P(1-Ad)$_2{}^n$Bu by stirring of the phosphines with 2 equiv of Se in $CDCl_3$ at 60 °C for 40 min. The resulting phosphine selenides formed quantitatively, and the coupling constants $^1J_{PSe}$ were measured without isolation. Interestingly, $^1J_{PSe}$ values obtained for $P^tBu_2{}^n$Bu (690 Hz) and P(1-Ad)$_2{}^n$Bu (680 Hz) are lower than that of P^tBu_3 (712 Hz),[57] indicating that the first two phosphines are more basic. This may imply that these ligands form more stable hydrido complexes **14** and **15** with respect to the P^tBu_3-ligated complexes. However, care must be taken in correlating $^1J_{PSe}$ constants with electronic properties of phosphines since $^1J_{PSe}$ also may depend on steric factors.[58] Thus, the poor reactivity of $P^tBu_2{}^n$Bu- and P(1-Ad)$_2{}^n$Bu-ligated hydrobromide complexes toward the amine bases as compared to **18** may be explained by both steric and electronic factors.

Palladium hydride complexes are assumed to be crucial intermediates in many palladium-catalyzed coupling reactions of aryl halides.[59] In general, the main role of base in these reactions consists of trapping the hydrogen halide from [Pd(H)-

(54) Most phosphine-containing palladium carbonyl clusters possesses from 3 to 69 palladium atoms: (a) Cavell, K. J. In *Comprehensive Organometallic Chemistry III*; Mingos, D. M., Crabtree, R. H., Canty, A., Eds.; Elsevier: Oxford, 2007; Vol. 8, pp 206−210. (b) Kudo, K.; Hidai, M.; Uchida, Y. *J. Organomet. Chem.* **1971**, *33*, 393. (c) Yoshida, T.; Otsuka, S. *J. Am. Chem. Soc.* **1977**, *99*, 2134. (d) Mednikov, E. V.; Eremenko, N. K.; Mikhalkov, V. A.; Gubin, S. P.; Slovokhotov, Y. L.; Struchkov, Y. T. *J. Chem. Soc., Chem. Commun.* **1981**, 989. (e) Goddard, R.; Jolly, P. W.; Krüger, C.; Schick, K.-P.; Wilke, G. *Organometallics* **1982**, *1*, 1709. (f) Manojloviæ-Muir, L.; Muir, K. W.; Lloyd, B. R.; Puddephatt, P. J. *J. Chem. Soc., Chem. Commun.* **1985**, 536. (g) Klein, H.-F.; Mager, M. *Organometallics* **1992**, *11*, 3915. (h) Tran, N. T.; Kawano, M.; Dahl, L. F. *J. Chem. Soc., Dalton Trans.* **2001**, 2731.

(55) At room temperature reaction does not occur due to very low solubility of TMEDA·HBr in toluene.

(56) (a) Allen, D. W.; Taylor, B. F. *J. Chem. Soc., Dalton Trans.* **1982**, 51. (b) Socol, S. M.; Verkade, J. G. *Inorg. Chem.* **1984**, *23*, 3487. (c) Suárez, A.; Méndez-Rojas, M. A.; Pizzano, A. *Organometallics* **2002**, *21*, 4611.

(57) Du Mont, W.-W.; Kroth, H.-J. *J. Organomet. Chem.* **1976**, *113*, C35.

(58) Pinnell, R. P.; Megerle, C. A.; Manatt, S. L.; Kroon, P. A. *Inorg. Chem.* **1973**, *95*, 977.

(59) Reviews on palladium hydride complexes: (a) Grushin, V. V. *Chem. Rev.* **1996**, *96*, 2011. (b) Hii, K. K. In *Handbook of Organopalladium Chemistry for Organic Synthesis*; Negishi, E. I., Ed.; Wiley-Interscience: New York, 2002; Vol. 1, pp 81−90.

(Hal)L_2] species to regenerate the active palladium(0) catalyst. The importance of such dehydrohalogenations was clearly illustrated by Fu and co-workers, who showed that the low catalytic activity of Pd/PCy_3 compared to Pd/P^tBu_3 in the Mizoroki−Heck vinylation of aryl chlorides is attributed to the formation of a stable hydrido palladium complex, [Pd(H)(Cl)$(PCy_3)_2$], that is reluctant to react with the base used in catalytic reaction.[60] In contrast, we observed here that the palladium-catalyzed formylation of aryl bromides displays a completely different trend: *the most efficient catalytic systems generate the most stable palladium hydride complexes* **14** and **15**. To ensure that these hydride complexes are relevant to catalysis, we further studied their generation and ability to catalyze the formylation. As shown above, hydrogenolysis of the acyl complex **8** in the presence of the base at 50 °C gave carbonyl cluster **17** as the only organometallic product (eq 17, Table 10, entry 6). In the presence of phosphine the reaction slowed down and a mixture of **14** and **17** was formed. The ratio **14** to **17** increased with increasing concentration of the phosphine ligand (Table 10, entries 6−8). At 100 °C the hydrobromide complex **14** was obtained as the major palladium-containing species, providing the phosphine ligand was added (eq 18). These results suggest that hydride complex **14** is not necessarily the direct product of hydrogenolysis, but a result of a subsequent transformation of carbonyl complex **17**. Indeed, **17** was completely transformed into **14** under conditions similar to those used for the catalytic reaction (toluene-d_8 solution, 1 equiv of phosphine, excess of TMEDA·HBr under CO/H_2 atmosphere at 100 °C for 16 h) (eq 21).

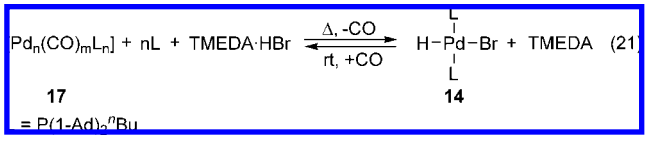

The $^{31}P\{^1H\}$ NMR spectrum of the filtered reaction mixture revealed disappearance of **17** and appearance of a singlet at 57.4 ppm belonging to the hydride species **14**. Additionally, the ^1H NMR displayed the characteristic high-field triplet at −13.2 ppm (J_{PH} = 7.9 Hz) corresponding to the hydride proton of **14**. Notably, this transformation is also reversible.[61] It is likely that interconversion between **14** and **17** occurs via the bisphosphine palladium complex **1**. In fact, **17** reversibly reacts with free ligand to give **1** (eq 16), which in turn reacts with TMEDA·HBr to give **14** (eq 19). Moreover, a mixture of [Pd$_n$(CO)$_m$L$_n$]/L catalyzed the test reaction, providing the same yield (87%) and selectivity (87%) as obtained with [PdL_2] (Table 11, entry 8).

Apparently, the carbonyl cluster [Pd$_n$(CO)$_m$L$_n$] serves as a [PdL_2] source for the catalytic reaction.[62] The same is true for the bromohydride complex [Pd(Br)(H){P(1-Ad)$_2$^{n}Bu}$_2$] (**14**). Although being "inert" toward the amine as shown by NMR, **14** is nevertheless able to generate highly reactive palladium(0) species in the presence of TMEDA. Hence, complex **14** catalyzed the formylation of 4-bromobenzotrifluoride to give the desired aldehyde in 87% yield, which is comparable (86%) to the original catalytic system comprising $Pd(OAc)_2$/P(1-Ad)$_2$^{n}Bu (Table 10, entry 7). Compound **14** also reacted with 4-bromobenzotrifluoride in the presence of 2 equiv of TMEDA in toluene-d_8 to give the oxidative addition product **6**. However, this reaction proceeded under more drastic conditions (>1.5 h at 100 °C) as compared to the oxidative addition of the respective palladium(0) complex **1** (1.5 h at 70 °C). The oxidative addition product **7** is not observed when **14** is heated with 4-bromobenzotrifluoride in the absence of base.[63] It appears that regeneration of palladium(0) from the palladium hydride species in the presence of the base and subsequent oxidative addition are the rate-determining steps. These transformations require at least 100 °C to proceed with reasonable rate, while all steps of the catalytic cycle from oxidative addition to hydrogenolysis occur at 70 °C or below. At the same time, the catalytic reaction was shown to proceed at 100 °C but not at 70 °C.

Table 11. Test of Isolated Complexes in Catalytic Reactions

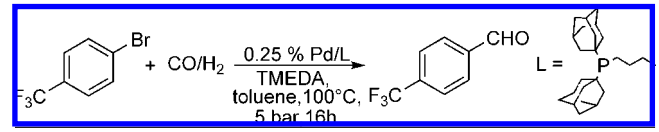

expt	complex	Pd/L ratio	conversion of ArBr, %[a]	yield of ArCHO, %[a]	selectivity, %
1	$Pd(OAc)_2$/L	1:3	100	86	86
2	[PdL_2] (**1**)	1:2	100	87	87
3	[Pd(Br)(Ar)L]$_2$(**3**)	1:1	94	80	85
4	[Pd(Br)(Ar)L]$_2$(**3**)/2L	1:2	100	85	85
5	[Pd(Br){C(O)Ar}L]$_2$(**8**)	1:1	93	82	88
6	[Pd(Br){C(O)Ar}L]$_2$(**8**)/2L	1:2	100	84	84
7	[Pd(Br)(H)L_2](**14**)	1:2	100	87	87
8	[Pd$_n$(CO)$_m$L$_n$](**17**)/nL^b	1:2	100	87	87

[a] Conversion and yield were determined by GC using hexadecane as internal standard. [b] The catalyst of this composition was obtained by bubbling CO via solution of [PdL_2] in toluene.

The data obtained for the stoichiometric studies on the formylation of aryl halides with Pd/P(1-Ad)$_2$^{n}Bu catalyst are summarized in Figure 16. An important point of the catalytic cycle is that hydride complex **14** and cluster compound **17** are considered as sources for catalytically active [PdL]/[PdL_2] species. Both complexes **14** and **17**, being in equilibrium, maintain the concentration of [PdL]/[PdL_2] at such a low level that oxidative addition becomes the rate-determining step of the reaction. Indeed, when the formylation of 4-bromobenzotrifluoride catalyzed by 1 mol % of **1** is stopped after 1.5 h at 61% conversion, the $^{31}P\{^1H\}$ NMR spectrum displayed three main resonances corresponding to **14**, **17**, and P(1-Ad)$_2$^{n}Bu in a 1.1:1:2.1 ratio.[64] In other words, complexes **14** and **17** are "reservoirs" of highly active [PdL] species, releasing them in low concentration throughout the reaction, thus making the Pd/P(1-Ad)$_2$^{n}Bu catalytic system highly efficient. The same is also true for the formylation catalyzed by $Pd/P^tBu_2{}^nBu$. The impor-

(60) Hills, I. D.; Fu, G. C. *J. Am. Chem. Soc.* **2004**, *126*, 13178.
(61) According to $^{31}P\{^1H\}$ NMR spectrum, the reaction of **14** with 4 equiv of TMEDA in toluene-d_8 at 5 bar pressure of CO/H_2 at room temperature after 16 h yielded a mixture of carbonyl compound **17**, free phosphine ligand, and starting complex **14** as indicated by three singlets in at 46.6, 24.4 and 57.4 ppm in a 1:1:4.65 ratio.
(62) Generally, in catalytic cycles of carbonylation reactions carbonyl palladium(0) complexes are postulated to be monomeric and considered as direct intermediates involved in oxidation addition. See for example: (a) Ozawa, F.; Kawasaki, N.; Okamoto, H.; Yamamoto, T.; Yamamoto, A. *Organometallics* **1987**, *6*, 1640. (b) Carpentier, J.-F.; Castanet, Y.; Mortreux, A.; Petit, F. *J. Organomet. Chem.* **1994**, *482*, 31.
(63) In contrast, recently Hartwig reported that oxidative addition of bromobenzene to hydride complex [Pd(Br)(H)(P^tBu_3)$_2$] proceeds even faster than to [Pd(P^tBu_3)$_2$], see ref 25.
(64) When the reaction was carried out with $Pd(OAc)_2$/P(1-Ad)$_2$^{n}Bu additional resonances were observed. These could be attributed to some complexes containing coordinated acetoxy ligand. See for example ref 65e.

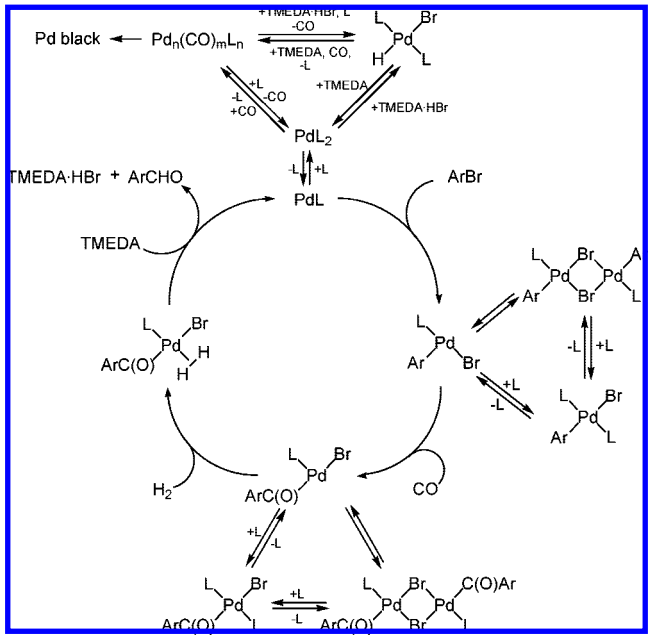

Figure 16. Proposed catalytic cycle for formylation of aryl bromides with $Pd/P(1\text{-}Ad)_2{}^nBu$.

tance of maintaining a low concentration of palladium(0) species for catalyst longevity can be rationalized as follows: the efficiency of the Pd(0) catalyst is dictated by competition of oxidative addition and decomposition via agglomeration of Pd(0) species, leading eventually to the formation of palladium black. The rate of this latter process is second order in Pd or higher, whereas oxidative addition is usually first order in palladium(0).[65] Therefore, catalyst systems maintaining concentration of active palladium(0) species on a low level during the respective reaction often possess prolonged existence.[66]

In contrast, the low activity of the Pd/P^tBu_3 system in the formylation of aryl bromides is attributed to formation of the poorly soluble complex [Pd(Br){C(O)Ar}(TMEDA)] (**16**). The low longevity of the Pd/P^tBu_3 catalyst is a consequence of the limited stability of the corresponding palladium(0) complexes in presence of base and carbon monoxide.

Conclusion

In summary, we report the first comprehensive study on the catalytic cycle of a palladium-catalyzed formylation of aryl halides with synthesis gas. This methodology has been recently applied by industry, and we have elucidated the mechanism of this synthetically useful reaction. More specifically, most relevant catalytic intermediates have been unambiguously characterized, and the synthesis and solution chemistry of complexes bearing $P(1\text{-}Ad)_2{}^nBu$, $P^tBu_2{}^nBu$ and P^tBu_3 ligands are described in detail. Using $Pd/P(1\text{-}Ad)_2{}^nBu$, the most efficient catalyst known to date for formylation of aryl bromides, we compared results of stoichiometric studies with those of the catalytic reaction. The data obtained imply that $[Pd_n(CO)_mL_n]$ (**17**) and [Pd(Br)(H)L_2] (**14**) are resting states of the active catalyst and probably may not lie within the catalytic cycle. During the reaction course, complexes **14** and **17** keep the concentration of the catalytically active species at a low level, which has two consequences: (1) oxidative addition of the aryl bromide becomes the rate-determining step of the reaction and (2) the high efficiency and longevity of the $Pd/P(1\text{-}Ad)_2{}^nBu$ catalyst system. Notably, the product-forming step, hydrogenolysis of the acyl complex $[Pd(Br)(p\text{-}CF_3C_6H_4CO)\{P(1\text{-}Ad)_2{}^nBu\}]_2$, is significantly accelerated by a base and occurs under mild conditions (25 °C, 5bar of CO/H_2), thus making the catalytic reaction in the presence of $Pd/P(1\text{-}Ad)_2{}^nBu$ feasible at lower pressures compared to all other previously reported catalysts. These conclusions are also valid for the catalyst comprising a similar unsymmetrical alkylphosphine ligand, $P^tBu_2{}^nBu$. Additionally, stoichiometric studies of the poorly active Pd/P^tBu_3 catalytic system led to the synthesis of the first stable three-coordinate neutral palladium acyl complex. This complex is less prone to hydrogenolysis as compared to $P(1\text{-}Ad)_2{}^nBu$- and $P^tBu_2{}^nBu$-ligated acyl complexes and, in the presence of amine base, gives a catalytically inactive diamine acyl complex, which results in poor performance of the Pd/P^tBu_3 catalyst in the catalytic formylation. Finally, this study led to elucidation of the special role of unsymmetrical trialkylphosphine ligands, which have been largely neglected in coupling chemistry.

Acknowledgment. This research was supported by the State of Mecklenburg-Vorpommern, the BMBF, the DFG (Leibniz Prize), and the Fonds der Chemischen Industrie (FCI). We thank Dipl. Ing. A. Koch and Ms. S. Giertz (LIKAT) for their excellent analytical and technical support.

Supporting Information Available: All experimental procedures and spectroscopic data of new compounds. This material is available free of charge via the Internet at http://pubs.acs.org.

JA804997Z

(65) See for example: (a) Fitton, P.; Rick, E. A. *J. Organomet. Chem.* **1971**, *28*, 287. (b) Fauvarque, F.-F.; Pflüger, F.; Troupel, M. *J. Organomet. Chem.* **1981**, *208*, 419. (c) Amatore, C.; Pflüger, F. *Organometallics* **1990**, *9*, 2276. (d) Hartwig, J. F.; Paul, F. *J. Am. Chem. Soc.* **1995**, *117*, 5373. (e) Amatore, C.; Carré, E.; Jutand, A.; M′Barki, M. A. *Organometallics* **1995**, *14*, 1818. (f) Alami, M.; Amatore, C.; Bensalem, S.; Choukchou-Brahim, A.; Jutand, A. *Eur. J. Inorg. Chem.* **2001**, 2675.

(66) (a) Beletskaya, I. P.; Cheprakov, A. V. *J. Organomet. Chem.* **2004**, *689*, 4055. (b) Dupont, J.; Consorti, C. S.; Spencer, *J. Chem. Rev.* **2005**, *105*, 2527.